Platinum sponsor

Celanese

2026 Implant Polymers:

UHMWPE & PEEK Conference

Wednesday & Thursday,
June 17 – 18, 2026

Bossone Research Enterprise Center,
Drexel University, Philadelphia, USA

Hosted by Drexel University and the University of Turin

CONFERENCE PROGRAM

Celanese

Additional Sponsors:

Gyroid

CeramTec
THE CERAMIC EXPERTS

Invibio
BIOMATERIAL SOLUTIONS

Orthoplastics
A VIANT COMPANY
science making a material difference

MITSUBISHI
CHEMICAL
GROUP
Mitsubishi Chemical Advanced Materials GmbH

Exponent

stryker

Organizers:

IRC
IMPLANT RESEARCH CORE

DREXEL UNIVERSITY
School of
Biomedical Engineering
and Science
College of Engineering and Computing

UNIVERSITÀ
DI TORINO

2026 Implant Polymers: **UHMWPE & PEEK Conference**

Wednesday & Thursday, June 17-18, 2026
Bossone Research Enterprise Center,
Drexel University, Philadelphia, USA

Hosted by Drexel University and the University of Turin

The purpose of the meeting is to bring together engineers, scientists, regulators, and clinicians from academia, industry, and government to present leading edge research on advancements in medical-grade UHMWPE, PEEK, and the rapidly growing field of polymer implant additive manufacturing technology. In addition to UHMWPE and PEEK, the Combined Meeting will also broadly showcase point-of-care additive manufacturing of implantable polymers.

Scientific and Organizing Committee and Invited Speakers:

Co-Presidents:	Pierangiola Bracco, Ph.D. & Steven Kurtz, Ph.D.
Organizer:	Hannah Spece, Ph.D.
Invited Speakers:	Matthew Di Prima, Ph.D.
	Ryan Roeder, Ph.D.
Panel Moderator & Members:	Ryan Siskey, M.S.
	Alan Porporati, Ph.D.
	John Bowsher, Ph.D.
	Ruth Heckler, M.S.
	Raelene Cowie, Ph.D.

Sponsorship

We are grateful for Celanese's Platinum Sponsorship of the 2026 Combined Meeting, as well as Silver Sponsorship from Gyroid LLC and Bronze Sponsorships from Invibio, Orthoplastics, Mitsubishi Chemical Advanced Materials, and CeramTec. Stryker Orthopaedics and Exponent sponsor our coffee breaks.

Wednesday, June 17, 2026 | Day One

Time	Subject	Presenter
7:00 AM	On Site Registration Opens, Breakfast Available	
8:00 AM	Opening Remarks	Steven Kurtz, Ph.D.
8:10 AM	Welcome	Amanda Dresch, B. A., Celanese

SESSION I: Clinical Performance of UHMWPE

Session Moderator: Steve Kurtz, Ph.D.

8:15 AM	**Podium Talk 1**: Innovation in Medical Implants Across Polymer Families	Victoria Black, B.S., Celanese
8:30 AM	**Podium Talk 2**: Volumetric Wear of Highly Cross-linked Polyethylene Sockets in Total Hip Arthroplasty Differs Across Brands: A Retrieval Study	PD Dr. med. Peter Wahl, University of Basel; University of Bern; Birshof Hospital, Muenchenstein
8:45 AM	**Podium Talk 3**: Spectroscopic Studies of UHMWPE Hip and Knee Explants Using XRD, UV-Vis, FT-IR, and ESR Techniques	MD Farhan Azim, B.S., University of Memphis
9:00 AM	**Podium Talk 4**: Polyethylene Wear in Reverse Total Shoulder Arthroplasty: Is Osteolysis at the Horizon?	Robin Pourzal, Ph.D., Rush University
9:15 AM	**Podium Talk 5**: From UHMWPE to Vitamin E-Stabilized HXLPE: Material-Driven Evolution and Clinical Survivorship of the Isoelastic RM Monoblock Acetabular Cup	Frank Eitel, M. Sc., Enovis
9:30 AM	**Podium Talk 6**: Nitrided Bearings Against Polyethylene	Michael Kurtz, Ph.D., Drexel University
9:45 AM	**Morning Coffee Break**	

SESSION II: UHMWPE in Alternative Bearing Pairs

Session Moderator: Ryan Siskey, M.S.

10:15 AM	**Podium Talk 7**: Regulatory Challenges in Predicting Wear Performance of Novel Bearing Surfaces for Orthopedic Devices	John Bowsher, Ph.D., U.S. Food and Drug Administration (FDA)
10:30 AM	**Podium Talk 8**: Evaluation of a Modern TiN-Coated Femoral Component: from Bench to Bedside	Ahmad Faizan, Ph.D., Stryker
10:45 AM	**Podium Talk 9**: Preservation of UHMWPE Wear Performance by ADLC-Coated Titanium Glenospheres Under High Demand Reverse Shoulder Conditions	Ruth Heckler, M.S., Enovis
11:00 AM	**Podium Talk 10**: Third Body Wear of an All-Polymer Total Knee Replacement	Raelene Cowie, Ph.D., University of Leeds

Wednesday, June 17, 2026 | Day One

Time	Subject	Presenter
11:15 AM	**Podium Talk 11**: Polyethylene Wear in Combination with Ceramic Femoral Components in Total Knee Replacement Under Standard and Abrasive Conditions	Alan Porporati, Ph.D., CeramTec
11:30 AM	**Podium Talk 12**: Abrasive Damage in Orthopedics: Test Methods Past, Present, and Future	Ryan Siskey, M.S., Exponent
11:45 AM	**Panel Discussion**: Abrasive Wear Test Methods for UHMWPE in Alternative Bearing Pairs	Moderator: Ryan Siskey Participants: Alan Porporati, John Bowsher, Ruth Heckler, Raelene Cowie
12:15 PM	**Rapid Fire Talks**: 3-minute presentations of selected UHMWPE posters	
12:30 PM	**Lunch and Poster Discussions**	

SESSION III: Oxidation in UHMWPE

Session Moderator: Pierangiola Bracco, Ph.D.

1:45 PM	**Podium Talk 13**: The Oxidation Resistance of UHMWPE Containing a Chemically Bonded Vitamin E Analog	Anuj Bellare, Ph.D., Polymerix Technologies
2:00 PM	**Podium Talk 14**: A Solution to Potentially Eliminate Oxidative Degradation and Enhance the Functional Performance of UHMWPE Liners in Artificial Joints	Prof. Dr. Rizwan Gul, University of Engineering and Technology, Peshawar, Pakistan
2:15 PM	**Podium Talk 15**:Free Radical Persistence and Oxidative Aging in Conventional and Vitamin E-Stabilized UHMWPE	Afsana Sharmin, M. S., University of Memphis
2:30 PM *Virtual*	**Podium Talk 16**: Lipid Peroxidation-Derived Aldehydes: A Novel Oxidation Pathway in UHMWPE Orthopedic Implants	Javier Poves, M.S., University of Zaragoza
2:45 PM	**Podium Talk 17**: Failure of Sequentially Annealed Highly Cross-linked UHMWPE Inserts – Is It Related to Oxidation?	Therese Bormann, Ph.D., Heidelberg University Hospital
3:00 PM	**Podium Talk 18**:Oxidation Study of Super Crosslinked Gradient UHMWPE	Zhangtao Zhang, Ph.D, b-ONE Ortho Corp
3:15 PM	**Afternoon Coffee Break**	

Wednesday, June 17, 2026 I Day One

Time	Subject	Presenter
3:15 PM	**Afternoon Coffee Break**	

SESSION IV: UHMWPE Properties, Processing, and Testing

Session Moderator: Anuj Bellare, Ph.D.

Time	Subject	Presenter
3:45 PM *Virtual*	**Podium Talk 19**: Wear Properties of Bupivacaine/UHMWPE Blends	Nicoletta Inverardi, Ph.D., Harris Orthopaedics Laboratory, Massachusetts General Hospital; Harvard Medical School
4:00 PM	**Podium Talk 20**: Annealing's Impact on the Microstructure and Mechanical Behavior of Vitamin E Containing Highly Crosslinked UHMWPE	Daniel Weller, Ph.D., Stryker Orthopaedics
4:15 PM	**Podium Talk 21**: A Novel Method for Measuring Residual Stress in Consolidated Implantable Grade UHMWPE	Katie Schindler, B .S., Mitsubishi Chemical Group
4:30 PM	**Podium Talk 22**: Thickness-Driven Normalization of UHMWPE Small Punch Test Results for Expanded ASTM F2977 Usability	Michael Tartaglia, B. S., Stryker Orthopaedics
4:45 PM	**Podium Talk 23**: Gentamicin Eluting UHMWPE as a Durable, Antimicrobial Spacer Material for Two Stage Revision Arthroplasty	Mehmet Asik, Ph.D., Harris Orthopaedics Laboratory, Massachusetts General Hospital; Harvard Medical School
5:00 PM	**Podium Talk 24**: Novel Spectroscopic Approaches for Oxidation Index Assessment in UHMWPE Implants	Azita HassanMazandarani M.S., Temple University
5:15 PM	**Day 1 Meeting Adjourns**	
7:00 PM	**Gala Dinner at Reading Terminal Market**	

Thursday, June 18, 2026 | Day Two

Time	Subject	Presenter
8:00 AM	**On Site Registration Opens, Breakfast Available**	

SESSION V: PEEK Bioactivity and Use in Devices

Session Moderator: Steve Kurtz, Ph.D.

Time	Subject	Presenter
9:00 AM	**Invited Talk 1**: Making PEEK Great Again: A HAPPE Journey from Concept to Commercialization	Ryan Roeder, Ph.D., University of Notre Dame; HAPPE Spine
9:30 AM	**Podium Talk 25**: BMSC Extracellular Matrix Formation on PEEK Lattices and a Collagen Membrane Interface	Fedra Zaribaf, MEng, Ph.D., Invibio Ltd, UK
9:45 AM	**Podium Talk 26**: Commercial Approval of a Fully Polymeric Surgical Mitral Valve	Ryan Stanfield, P.E.,Ph.D., University of Utah; Foldax, Inc.
10:00 AM	**Podium Talk 27**: Is Point of Care 3D Printing of PEEK Triflange Cups Feasible for Revision THA?	Steve Kurtz, Ph.D., Drexel University
10:15 AM	**Podium Talk 28**: CFR-PEEK in Orthopaedic Implants: What the Clinical Evidence Supports, What It Still Can't Answer, and How Evidence is Translated Into Use	Sherri Gambill, B.S., Invibio
10:30 AM	**Rapid Fire Talks**: 3-minute presentations of selected PEEK posters	
10:45 AM	**Morning Coffee Break and Poster Discussions**	

SESSION VI: 3D Printing at the POC and Characterization of 3DP PAEKs

Session Moderator: James Smith, Ph.D.

Time	Subject	Presenter
11:30 AM	**Invited Talk 2**: 3D Printed PAEK Implants and the Road to Point of Care Printing	Matthew Di Prima, Ph.D., U.S. Food and Drug Administration (FDA)
12:00 PM	**Podium Talk 29**: The Road Towards Establishing Clinical Services to Develop and Produce Patient-Specific PAEK Implants in and by the Healthcare Facility at Point-of-Care: the Singapore General Hospital Experience	Mark Tan Bangwei, MBBS, MRCS, FRCR, Singapore General Hospital
12:15 PM	**Podium Talk 30**: Evaluating the Static Mechanical Performance of Fused Filament Fabricated Anterior Lumbar Interbody Fusion PEKK and PEEK Devices	Abigail Tetteh, Ph.D., Drexel University; Exponent Inc.
12:30 PM	**Podium Talk 31**: What Drives the Protein Adsorption of 3D Printed PAEK Polymers?	Paul DeSantis,M.S., Drexel University
12:45 PM	**Podium Talk 32**: Optimization of FFF Process Parameters for Compressive Properties of Solid and Porous Si3N4-PEEK	Tabitha Derr, M.S., Drexel University
1:00 PM	**Closing Remarks and Meeting Adjourn**	Steven Kurtz, Ph.D.

2026 Implant Polymers: **UHMWPE & PEEK Conference**

Poster Presentations | **UHMWPE** | Day One

Title	Presenter
Effect of Chlorine Dioxide Terminal Sterilization on the Mechanical and Chemical Properties of UHMWPE Used in Total Joint Arthroplasty	Michael Tartaglia, B. S., Stryker Orthopaedics
Inflammatory Responses to Fine Wear Particles from Conventional and Highly Crosslinked Polyethylene Inserts	Robin Pourzal, Ph.D., Rush University
Influence of Terminal Sterilization Modality on Oxidative and Mechanical Properties of Crosslinked UHMWPE	Ruth Heckler, M.S., Enovis
Design of Hydroxyapatite Whisker Reinforced Polyetheretherketone Scaffolds for Bone In-Growth and Mechanical Integrity in Orthopedic Devices	Luis Vega Lugo, B.S., University of Notre Dame
In Vitro Apatite-Forming Ability of Hydroxyapatite Whisker Reinforced Polyetheretherketone	Elizabeth O'Connell,B.S., University of Notre Dame

Poster Presentations | Peek | Day Two

Title	Presenter
Computational Modeling to Assess the Influence of Geometric Variations on the Axial Compressive Performance of PEKK and PEEK Lumbar Spinal Cages	Abigail Tetteh, Ph.D., Drexel University; Exponent Inc
Using Sulfonation to Alter Surface Properties of 3D Printed PAEK Polymers	Paul DeSantis, M.S., Drexel University
Fatigue Strength of Additively Manufactured PEEK and Si3N4-PEEK Cervical Cages	Tabitha Derr, M.S., Drexel University
Effects of Hydrothermal Aging on the Flexural Properties of PEKK and LM-PAEK	Jasmine Johnson, B.S., Drexel University
Biomechanical Evaluation of Carbon Fiber-Reinforced Polyether Ether Ketone (CFR-PEEK) versus Titanium Plates for Fixation of High Tibial Osteotomy	Sherri Gambill, B.S., Invibio

SPECIAL THANKS
to all the sponsors & attendees at the 2026 Conference!

Platinum Sponsor: Celanese
Silver Sponsor: Gyroid LLC
Bronze Sponsors:
Orthoplastics
Invibio
Mitsubishi Chemical Advanced Materials
CeramTec GmbH

Coffee Breaks: Exponent and Stryker Orthopaedics

Interested in sponsoring our 2028 edition?
Please contact Steve Kurtz - skurtz@drexel.edu.

Volumetric wear of highly cross-linked polyethylene sockets in total hip arthroplasty differs across brands: a retrieval study

Wahl, P[1,2,3], Porrati, V[4,5], Schläppi, M[6], Kuttner, H[7], Sax, F[8], Resl, MH[9], Simon, S[10,11], Hackl, K[10], Winkelmann, M[12], von Lewinski, G[13], Terhune, EB[4], Heuberger, R[14], Hall, DJ[4], Pourzal, R[4]

[1] University of Basel, Basel, Switzerland, [2] University of Bern, Bern, Switzerland, [3] Birshof Hospital, Muenchenstein, Switzerland, [4] Rush University Medical Center, Chicago, Illinois, [5] Polytechnic University of Milan, Milan, Italy, [6] Cantonal Hospital Winterthur, Winterthur, Switzerland, [7] Cantonal Hospital Chur, Chur, Switzerland, [8] Orthopaedic Clinic Markgroeningen, Markgroeningen, Germany, [9] Charité University Medicine Berlin, Berlin, Germany, [10] Orthopaedic Hospital Vienna-Speising, Vienna, Austria, [11] Medical University of Vienna, Vienna, Austria, [12] Cantonal Hospital Frauenfeld, Frauenfeld, Switzerland, [13] Hannover Medical School, Hannover, Germany, [14] RMS Foundation, Bettlach, Switzerland

peter.wahl@faculty.unibe.ch

Introduction: Wear and the related inflammatory tissue reactions remain limiting factors in long-term outcomes after total hip arthroplasty (THA). Although modern materials, such as highly cross-linked polyethylenes (HXLPE), mitigated the issue by reducing volumetric wear and consecutively also revision rates, it may just have been postponed, particularly as HXLPE produce smaller and biologically more active particles than conventional polyethylene. Furthermore, there are major differences among the various HXLPE bearings available on the market regarding wear resistance, and possibly also regarding associated revision rates over time. This study aimed at quantifying volumetric wear on components retrieved at revision from various brands, in relation to known and suspected clinical risk factors.

Methods and Materials: Intermediate analysis of an ongoing, multicentric study of HXLPE sockets collected at THA revision. Volumetric wear was quantified using a 5-axis optical coordinate measuring machine (RedLux, OrthoLux, Romsey, UK). Patient-related factors (such as age, height, weight, American Society for Anesthesiology (ASA) class), implant-related factors (diameter of the bearing, head material, brand) and orientation of the components (inclination and anteversion of the cup, antetorsion of the stem) were integrated into the analysis.

Results: As of 30.06.2025, 104 HXLPE THA cups/inlays were available. Of these, 79 could be analysed, after excluding those with deformation or retrieval damage too severe for reliable measurements. The median (range) time in situ was 8.7 (2.1 to 22.1) years. The median (range) wear volume and volumetric wear rate were 91 (1 to 674) mm^3 and 9 (0 to 130) mm^3/year, respectively (Fig. 1). Highcross (n = 56, Medacta, Castel San Pietro, Switzerland) showed approximately five times more wear ($p < 0.001$) than Durasul (n = 17, Zimmer Biomet, Zug, Switzerland). The median linear wear rate for Highcross was 27.4 µm/year and 11.7 µm/year for Durasul. While there was overall an excellent correlation ($R^2 = 0.94$) between linear and volumetric wear, this must be considered with caution, because retrievals with high wear had a large impact on this statistical analysis, whereas low wear retrievals showed very high variability (Fig. 2). The other brands (n = 6) were too small in group size at this stage of the study. Differences in wear were mostly driven by the brand, while other parameters (time in situ, ASA class, and weight) had only a minor impact.

Discussion: This is the first retrieval study comparing volumetric wear of HXLPE bearings retrieved at THA revision among various brands. Major differences in wear behaviour could be identified among brands. Particularly, differences in HXLPE processing appear to be the main determinant of wear. Respectively, one of the main HXLPE brands appears to have erratic wear behaviour, largely differing from the other ones. THA with this bearing also appears to have increased revision rates in various national registries. As the cohort grows, the analysis will be refined, integrating further parameters and brands.

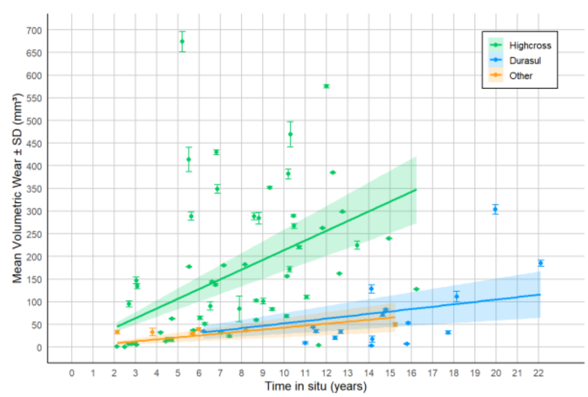

Fig. 1 – Volumetric wear over time.

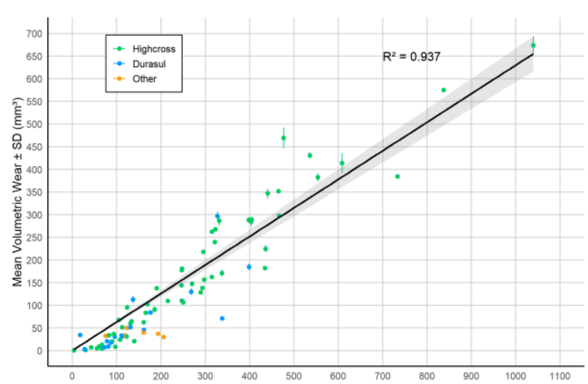

Fig. 2 – Relation between linear wear (extracted from the 3D wear maps) and volumetric wear.

Spectroscopic Studies of UHMWPE Hip and Knee Explants Using XRD, UV-Vis, FT-IR and ESR Techniques

Md Farhan Azim[1], Afsana Sharmin[1], Hannah Spece[2], Steven Kurtz[2], Muhammad Shah Jahan[1]
[1]Department of Physics and Material Science, The University of Memphis, Memphis, TN 38152, USA
[2]Drexel University, 3141 Chestnut St, Philadelphia, PA 19104
mazim@memphis.edu

Introduction: In 2019, Global Burden of Disease (GBD) reported that approximately 1.7 billion people globally live with unstable musculoskeletal conditions, that lead to disability worldwide [1]. This is expected to further increase as the global population ages with respect to time. Young people are also being affected by joint affections. Orthopedic joint replacements such as shoulder, ankle, elbow and specially hip, knee are broadly reported to improve restoring joint function, mitigating pain which essentially help to have a better quality of life [2, 3]. Ultrahigh molecular weight polyethylene (UHMWPE) is one of the arthroplasties polymeric materials that has received recognition in the field of joint replacement applications in the last 50 years. The cross-linked UHMWPE implants were first introduced in 1998 through continuous research with the intention of reducing the wear rate and oxidative degradation effect [4]. The formulation of cross-linked structure of UHMWPE after irradiation has made it possible to overcome those critical issues [5]. Again, studies of vitamin E antioxidants blending (pre-irradiation) or infusing (post-irradiation) have been undergoing over the past years to improve the degradation properties of implant/explant UHMWPE. In the literature, strong correlations between the oxidative degradation, degree of crystallinity and microhardness of UHMWPE were investigated, where higher oxidation index led to observe greater degree of crystallinity [6]. Conventional UHMWPE explants are more susceptible to oxidation without heat treatment. They have higher degrees of crystallinity and E-Modulus values after the air ambient gamma irradiation sterilization [7]. Another study shows that the maximum formulation of cross-linked UHMWPE can be possible through the optimal radiation dose level at low oxygen atmospheric condition. Even though this optimal value is not constant but can vary depending on the quality of UHMWPE such as 25, 50 or 100 KGy [8]. Remelting the irradiated UHMWPE can significantly decrease the number of free radicals where recombination process helps to build up the cross-linked structure of UHMWPE [9]. Studies regarding the number of long lived free radicals of explant UHMWPE in ambient temperature under open air atmosphere has not been done in the literature so far. The results in vivo performance of explants could benefit the manufacturing processes of UHMWPE such as radiation doses, remelting or vitamin E incorporation. This comprehensive study underscores the free radicals and oxidative degradation behavior of explant hip and Knee UHMWPE samples based on implantation site in vivo.

Methods and Materials: The retrieved solid UHMWPE samples were provided by the University of Drexel, Philadelphia, USA. The hip cups (longevity) were first introduced to the irradiation technique and then were undergone through the remelting process. The Knee as E1 parts were first irradiated and then vitamin E was infused. Vivacit-E knee samples were first blended through vitamin E, after that the irradiation process was done. These were implanted in vivo for specific time durations and retrieved because of failure issues. These explants were trimmed with 4 mm length, 2 mm width and 1 mm thickness each and preserved in open air atmosphere at room temperature. The semi-crystalline properties of UHMWPE samples were analyzed from X-ray diffractometer (XRD). Fourier Transform Infrared (FTIR) spectroscopy was used to identify the functional groups and molecular vibrations present in the samples. The presence of chemical compositions and band gap energy of the samples were determined from the UV-Vis spectroscopy measurement. Free radical concentrations (Spin/g) and different types of radicals were determined by using Electron Spin Resonance (ESR) technique.

Results: The XRD results for both hip and knee respectively revealed the orthorhombic structure of UHMWPE. The average crystallite size and degree of crystallinity were calculated for each explant. The FTIR peak signals for both hip and knee revealed the presence of C-H deformation, methylene group $-(CH_2)_n-$, C=O carbonyl and O-H functional groups. Oxidation index for knee and hip was calculated to analyze the degradation over the period in vivo. The presence of chemical compositions such as ketone, aldehyde, ester from these hip and knee samples was investigated from the UV-Vis measurement. The band gap energies obtained from the Tauc plots of knee and hip were measured Noticeably, no ESR signal was detected from the hip (longevity) samples. In contrast, left over of free radicals was confirmed in knee as vivacity-E and E1 samples from ESR signals over the period of time.

Discussion: Vitamin E in knee joints reacted with the radicals required to form cross-links during irradiation, resulting in lower cross-link density for vivacit-E. In E1, cross-linking happened before the Vitamin E was infused. Longevity hip cups contain robust cross-linking, but the post-irradiation remelting process slightly might relax some of C-H bonds compared to the irradiated E1. The ESR signals in vivacity-E and E1 suggested the presence of different types of alkyl, allyl, polyenyl or vitamin E radicals were still trapped inside the crystalline region, which is likely due to increased wear and oxidative stress from the more dynamic loading conditions experienced in the knee joint during ambulation. This mechanical load can enhance the diffusion of oxygen into the polymer matrix, accelerating oxidative degradation, which is further corroborated by the greater oxidation index observed for the knee as vivacit-E and E1 in FTIR analysis compared to the longevity hip samples. The slightly lower band gap energy for vivacit-E and E1 as compared to longevity from UV-Vis measurements also might indicate that the polymer's electronic transition (π-π*) was altered, potentially due to chain scission that occurs under such stress. Vivacit-E and E1 knee parts retained greater degree of crystallinity over longevity hip cups as observed in XRD results, because those were never melted. These findings of UHMWPE's behavior in joints contribute to guiding future advancements in orthopedic materials.

XRD results

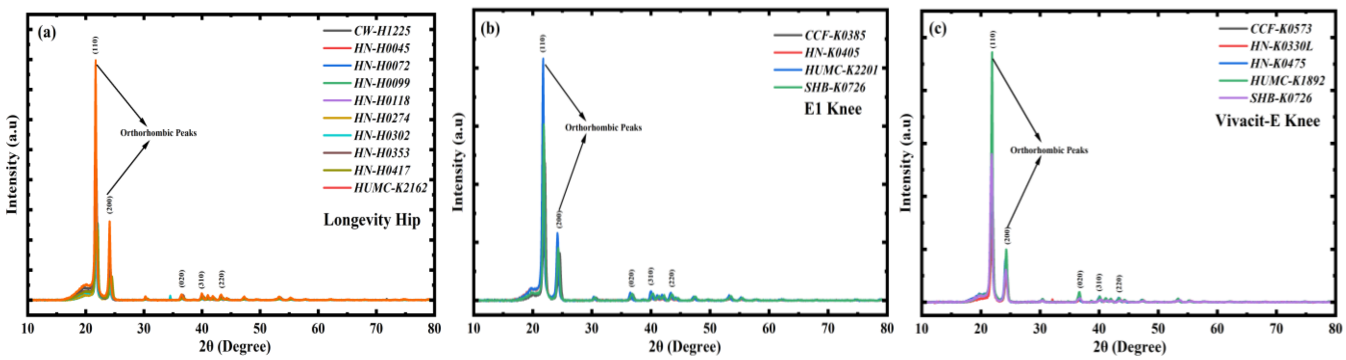

FTIR results

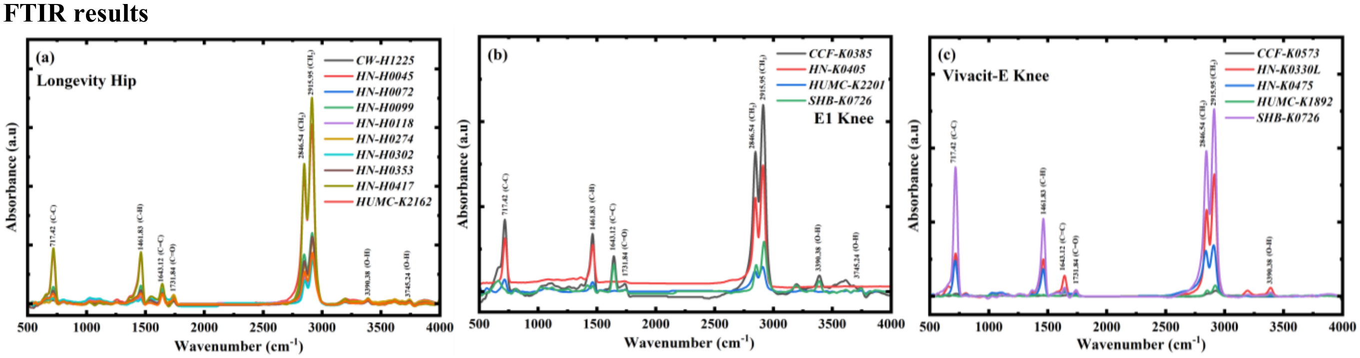

UV-Vis Results

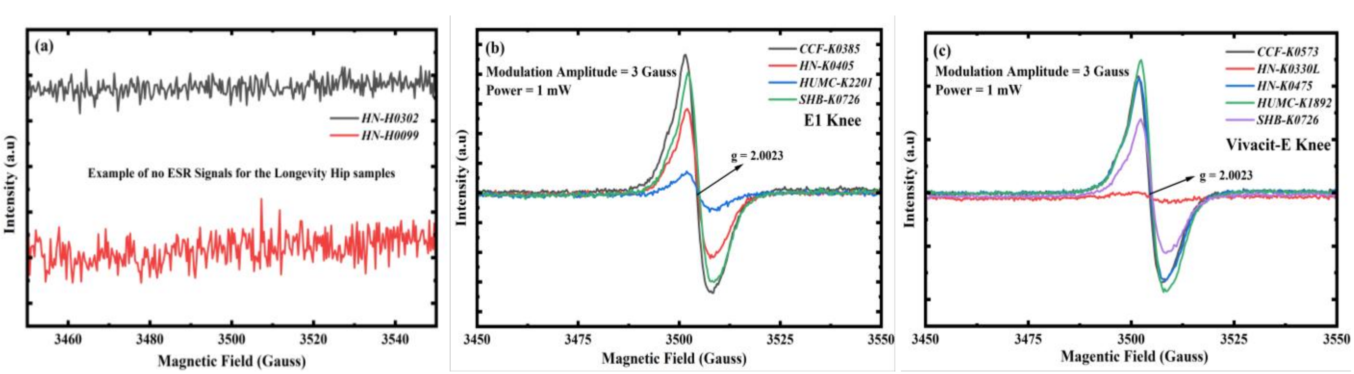

ESR results

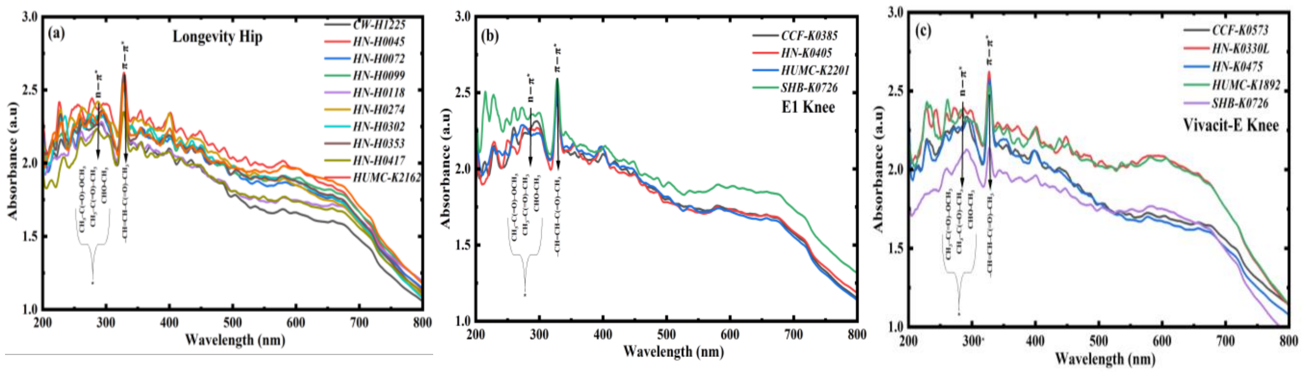
(a)
Longevity Hip
CW-H1225
HN-H0045
HN-H0072
HN-H0099
HN-H0118
HN-H0274
HN-H0302
HN-H0353
HN-H0417
HUMC-K2162
Absorbance (a.u)
Wavelength (nm)
(b)
CCF-K0385
HN-K0405
HUMC-K2201
SHB-K0726
E1 Knee
Absorbance (a.u)
Wavelength (nm)
(c)
CCF-K0573
HN-K0330L
HN-K0475
HUMC-K1892
SHB-K0726
Vivacit-E Knee
Absorbance (a.u)
Wavelength (nm)

Polyethylene wear in reverse total shoulder arthroplasty: Is osteolysis at the horizon?

Remi E. Ben-Davies, Jennifer L. Wright, Deborah J. Hall, Julia Hochstatter Gregory P. Nicholson, Grant E. Garrigues, Robin Pourzal

Disclosures: GP Nicholson (1-Anika, Innomed, Styker; 2-Arthrosurface; 3B-AzurMed, Stryker; 9-ASES), GE Garrigues (1-DJO, Tornier; 2-DJO; 3B-DJO, Mitek, Restor3d, Tornier; 4-Aevumed, Cultivate MD, Genesys, Patient IQ, Restor3d, ROM 3, Sparta Biopharma; 6-DJO, 7B- Elsevier; 8-JSES; 9-AOS, ASES, AANA), Robin Pourzal (5-Enovis, CeramTec, Zimmer Biomet)

Background:
Reverse total shoulder arthroplasty (rTSA) is among the most common surgical interventions to alleviate pain and restore function in patients with glenohumeral joint disease. All rTSAs use a spherical metal glenosphere that articulates with a polyethylene (PE) liner to restore motion and provide joint stability. In the hip, PE wear was shown to cause inflammatory tissue responses, often resulting in osteolysis and implant failure. However, there is limited understanding of the effect of PE wear in the rTSA. This study aimed to quantify PE wear and characterize associated wear scars from normally articulating rTSA humeral liners. The corresponding periprosthetic tissue was analyzed for PE presence and tissue response.

Methods:
Initially, 50 PE rTSA liners with periprosthetic tissue were available (retrieved between 2017 and 2023). Of these, 26 were in situ for 2 years or greater, with a mean of 4.6 years (95% CI, 3.4, 5.8). Wear volume and wear scars were quantitatively assessed using an optical coordinate-measuring-machine (RedLux). Wear was qualitatively assessed with a wear score (range: 1-14). Histological sections were prepared for H&E staining and Fourier transform infrared spectroscopy imaging (FTIR-I). The presence of macrophages was semi-quantitatively scored (1-mild to 4-severe). FTIR-I (Agilent) was conducted to generate chemical images of intracellular PE particle accumulation. Statistical analysis included Pearson's and Spearman's correlation.

Results: The median wear score across 26 liners was 4 (min. 1, max. 10). The macrophage scores were 1-minimal (N=1), 2—mild (N=4), 3-moderate (N=6), and 4-severe (N=15). Wear volume could only be assessed for 13 liners after excluding those with severe removal damage or excessive rim damage caused scapular notching. Ultimately, wear could only be quantified for nine cases. For the remaining liners, wear had not progressed enough to be detectable. The mean (± standard deviation) wear volume of the remaining liners was 73.4 (±59.5) mm^3, and the median (min., max.) wear volume was 44.5 (28.5, 210.3) mm^3, respectively. The mean and median volumetric wear rates (VWR) were 19.4 (± 16.6) mm^3 and 10.8 (7.29, 52.3) mm^3, respectively. The PE wear volume and rate did not correlate with wear score nor macrophage score. Wear rate correlated positively with a higher incidence of aseptic loosening ($p=0.043$). Heat maps indicated the maximum wear was generally located in the inferior-anterior region of the bearing surface. Three wear scars appeared symmetrical and offset from the center; two had a kidney shape, two indicated edge loading, and two indicated a shift in wear scar location. FTIR-I analysis showed PE particle accumulation in five cases. Intracellular PE accumulation correlated positively with time in situ ($p=0.02$).

Discussion:
Our results suggested a lower volume wear rate (VWR) compared to previous studies. The only other CMM study reported a wear volume range of 42.5 to 89.2 mm^3 in a study of four liners with 470 mm^3/year as the maximum wear rate. Another found the mean VWR of 114.5±160.3 mm^3/year across 32 liners using microCT [2] and 42±22 mm^3/year across 13 liners utilizing radio stereometric analysis. However, our study excluded liners with rim damage caused by scapular notching, as this wear model results from unintended contact conditions, leading to mechanical failure. Our focus is on wear generated during normal articulation and the associated PE wear that may result in inflammatory tissue responses and ultimately osteolysis. The shape of the wear scar varied among the liners, which may be related to patient activities, range of motion, and surgical implant alignment. Tissue analysis found a strong tissue response in most cases, and intracellular PE accumulation over time. Our study cohort was too small, and implantation duration was too short to establish a relationship between wear and tissue response.

[1] Lewicki, K.A. et al. JOR, 35(5): 980-987 (2017); [2] Kurdziel, M.D. et al. JOR, 36(7): 2007-2014 (2018); [3] Van de Kleut et al. JSES, 29: 695-1702 (2020); [4] Liu et al. Biotribology, 26 (2021); [5] Liu et al. APMIS, 132(8): 553-563 (2024) [6] Godoy et al., ORS 2025

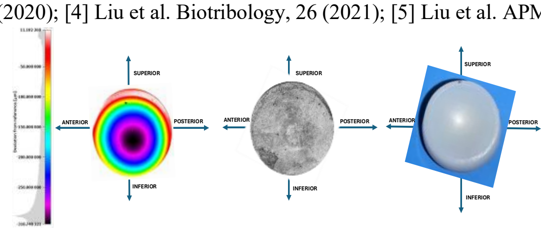

Figure 1 Example of a heat map (left) generated from CMM data. This liner features a wear scar concentrated in the inferior-anterior quadrant of the bearing surface. The light intensity map (middle) and corresponding photo (right) of the liner provide additional context

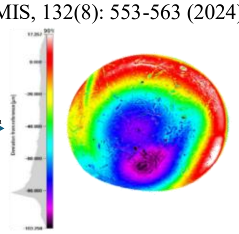

Figure 2 Heat map of a liner that experiences two overlapping, distinct wear scars, indicating a sudden shift, possibly due to dislocation or loosening.

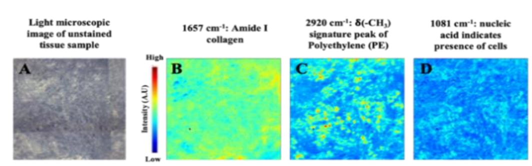

Figure 3 A) Light micrograph of unstained joint capsule tissue. FTIR-I chemical images at various wavenumbers show the presence of B) Amide I (collagenous tissue), C) accumulation of fine PE particles, D) phosphates indicative of nucleic acid (macrophages). PE particle-laden macrophages are present based on the overlap between C) and D).

From UHMWPE to Vitamin E-Stabilized HXLPE: Material-Driven Evolution and Clinical Survivorship of the Isoelastic RM Monoblock Acetabular Cup

Eitel, Frank[1], Johnson, James[1,2], Heckler Ruth[1], Heinrichs, Christian[1], May, Viola [1], Drew, Alex[1]
[1]Enovis AG, Bettlach Switzerland; [2]Colorado State University, Fort Collins, CO frank.eitel@enovis.com

Introduction: The RM monoblock acetabular cup provides a useful case study in polyethylene-driven implant evolution in primary total hip arthroplasty (THA). The platform was originally conceived as an isoelastic, uncemented all-polyethylene acetabular component intended to more closely approximate cancellous bone than conventional metal-backed shells, with the aim of promoting physiologic load transfer, reducing stress shielding, and eliminating the liner-shell interface associated with backside wear[1–3]. Across successive generations, the core monoblock concept with titanium particle coating was preserved while the principal changes occurred first in fixation strategy and geometry, from the peganchored RM Classic to the equatorial press-fit RM Pressfit, and later in polymer formulation with the introduction of vitamin E-stabilized highly crosslinked polyethylene (VE-HXLPE) in RM Pressfit vitamys[1–3]. This narrative review therefore examines the RM cup not simply as a chronological product evolution, but as a biomaterials question: whether these generational changes, particularly the transition from conventional UHMWPE to VEHXLPE, translated into measurable improvements in wear, fixation, and long-term clinical performance.

Methods and Materials: A focused narrative literature review was performed using long-term cohort studies, randomized comparative trials, a recent systematic review, and 2025 national registry reports describing RM Classic, RM Pressfit, and RM Pressfit vitamys (Mathys Ltd. [Enovis], Bettlach, Switzerland) constructs in primary [1–13], and patientreported function.

Results: The material rationale has remained consistent across generations. UHMWPE and VEHXLPE used in the RM cup have elastic moduli reported around 1000 and 800 MPa, respectively, much closer to cancellous bone (approximately 5006000 MPa) than titanium [105 GPa], supporting the isoelastic objective of more physiologic acetabular load transfer [1]. In a randomized trial, the RM Pressfit vitamys cup preserved significantly more periacetabular bone than a modular titanium pressfit cup, including less polar bone loss at 2 years (4.9% vs 15.9%, $p = 0.005$) [2]. The 2025 systematic review of 12 studies (1491 hips; mean follow-up 8.1 years) reported overall survivorship of 82.7%100%, aseptic loosening-free survivorship of 94.4%-100%, mean postoperative Harris Hip Score of 92.6, supporting the durability of the broader RM isoelastic concept [3].

The RM Classic established the long-term viability of monoblock polyethylene fixation, with 20-year follow-up showing 94.4% survivorship for aseptic loosening [3,4]. Registry-based generational analysis of 13272 RM cups found comparable all-cause revision rates across RM Classic, RM Pressfit, and RM vitamys (revision rates were similar in all groups (between 0.57 and 0.63%), with fewer revisions for acetabular loosening and dislocation in the vitamys group, although follow-up remained shorter for the most recent generation[1]. The RM Pressfit generation preserved the same isoelastic monoblock philosophy while shifting to equatorial press-fit fixation and polar flattening; 5- to 10.5-year follow-up studies reported survivorship of 96.1%100%, wear of 0.058-0.09 mm/year, and low cup migration [3,5,6]. The most consequential material step occurred in 2009 when UHMWPE was replaced by VE-HXLPE. Randomized trials demonstrated lower femoral head penetration and approximately 66% lower steady-state wear for vitamys versus conventional UHMWPE at 5 years, with significantly less wear also maintained at 6 years [3,7,8]. Ten-year vitamys cohorts now report 95.5%98% survivorship, 100% survivorship for aseptic loosening, Harris Hip Score or modified Harris Hip Score around 93-95, and no radiographic osteolysis or loosening[3,9,10]. These cohort findings are reinforced by current national registries: revision probability for optimys (cementless, calcar-guided, curved short-stem prosthesis)/RM Pressfit vitamys THA constructs was 2.8% at 10 years in Australia, 2.1% at 10 years in Germany, and 2.8% at 12 years in Switzerland, each lower than the corresponding national averages for comparable uncemented THA constructs [11–13].

Conclusion: Across five decades, the RM cup lineage illustrates selective evolution of an isoelastic monoblock concept in which fixation mechanics changed first and polyethylene formulation changed later, while the underlying bone-matched design rationale remained constant[1,3]. The most clearly material-associated advance is the transition from conventional UHMWPE to vitamin E-stabilized HXLPE, which has been associated with lower femoral head penetration and reduced steady-state wear in comparative studies while preserving the favorable bone-preserving and low-wear characteristics of the monoblock construct. At the same time, the available literature does not fully isolate the independent effect of polyethylene formulation from other generational differences, including follow-up duration, femoral head size, and era-related changes in fixation and practice patterns, and registry analyses suggest that all-cause revision rates across RM generations remain broadly comparable[1,3]. Taken together, the evidence supports the

RM monoblock acetabular cup as a durable polyethylene-based acetabular technology and suggests that the later material evolution to VEHXLPE strengthened the tribological performance
1,3,9
.

References:

1. Foxall-Smith M, Wyatt MC, Frampton C, Kieser D, Hooper G. The 45-year evolution of the Mathys RM monoblock cups: have the paradigm shifts been worthwhile? HIP International. 2023;33(2):193-202. doi:10.1177/11207000211067507

2. Brodt S, Jacob B, Nowack D, Zippelius T, Strube P, Matziolis G. An Isoelastic Monoblock Cup Retains More Acetabular and Femoral Bone Than a Modular Press-Fit Cup: A Prospective Randomized Controlled Trial. J Bone Joint Surg Am. 2021;103(11):992-999. doi:10.2106/JBJS.19.00787

3. Longobardi V, Minelli M, Pietrogrande G, Anzillotti G, Della Rocca F, Loppini M. Outcomes of Iso-Elastic Acetabular Cup in Primary Total Hip Arthroplasty with 5-Year Minimum Follow-Up: A Systematic Review. J Clin Med. 2025;14(18):6621. doi:10.3390/jcm14186621

4. Ihle M, Mai S, Pfluger D, Siebert W. The results of the titanium-coated RM acetabular component at 20 years: a long-term follow-up of an uncemented primary total hip replacement. J Bone Joint Surg Br. 2008;90(10):1284-1290. doi:10.1302/0301-620X.90B10.20274

5. Wyss T, Kägi P, Mayrhofer P, Nötzli H, Pfluger D, Knahr K. Five-year results of the uncemented RM pressfit cup clinical evaluation and migration measurements by EBRA. J Arthroplasty. 2013;28(8):1291-1296. doi:10.1016/j.arth.2012.11.004

6. Portet A, Besnard M, Ratsimbazafy C, Berhouet J, Samargandi R, Le Nail LR. The RM Press fit cup™: an investigation in 182 hips at ten-year follow-up. Orthop Traumatol Surg Res. 2025;111(8):103988. doi:10.1016/j.otsr.2024.103988

7. Rochcongar G, Remazeilles M, Bourroux E, et al. Reduced wear in vitamin E-infused highly cross-linked polyethylene cups: 5-year results of a randomized controlled trial. Acta Orthop. 2021;92(2):151-155. doi:10.1080/17453674.2020.1852785

8. Massier JRA, Van Erp JHJ, Snijders TE, Gast AD. A vitamin E blended highly cross-linked polyethylene acetabular cup results in less wear: 6-year results of a randomized controlled trial in 199 patients. Acta Orthop. 2020;91(6):705-710. doi:10.1080/17453674.2020.1807220

9. Haefeli PC, Zwahlen ZM, Baumgärtner R, Link BC, Beck M. RM Pressfit vitamys: the 10-year follow-up. Hip Int. 2025;35(2):142-149. doi:10.1177/11207000241304659

10. van Erp JHJ, Erisen H, Snijders TE, Bekkers JEJ, de Gast A. An acetabular component made from highly cross-linked polyethylene enriched with vitamin E: 10-year clinical results and wear rates. J Orthop. 2026;71:48-53. doi:10.1016/j.jor.2025.08.021

11. Lewis P, Gill D, McAuliffe M, et al. Hip, Knee and Shoulder Arthroplasty: 2025 Annual Report. Hip, knee and shoulder arthroplasty: 2025 Annual Report. October 1, 2025. doi:https://doi.org/10.25310/mxfr3061

12. Annual Report of the SIRIS Registry Hip & Knee, 20122024. Published online 2025. https://www.anq.ch/wpcontent/uploads/2025/12/ANQakut_SIRIS_Hips-Knee_Report_2025.pdf

13. Endoprothesenregister Deutschland (EPRD). 2025 Annual Report. Published online 2025.

Figure 1. Generational evolution of the RM monoblock acetabular cup, from RM Classic (1983) to RM Pressfit (2002) and RM Pressfit vitamys (2009).

Preservation of UHMWPE Wear Performance by ADLC-Coated Titanium Glenospheres Under High Demand Reverse Shoulder Conditions

Heckler, R[1], Johnson, J[1,2], Drew, A[1], Weisenburger, J[4], Siskey, R[3], Hall P [3] Plata, N[1], Haider, H[4]
[1]Enovis, Austin, TX, USA
[2]Colorado State University, Fort Collins, CO, USA
[3]Exponent, Philadelphia, PA, USA
[4]Department of Orthopaedic Surgery and Rehabilitation, University of Nebraska Medical Omaha, NE USA
Ruth.Heckler@enovis.com

Introduction: Polyethylene bearing performance remains a key determinant of long-term arthroplasty success, particularly when counterface damage or third-body challenge increases wear under adverse conditions. Surface technologies that maintain a favorable articulating counterface after abrasion may help preserve UHMWPE performance, but this depends on resisting progressive surface deterioration during high-demand use. The aim of this study was to evaluate whether a proprietary ADLCcoated titanium glenosphere can preserve UHMWPE wear performance under clean and abrasive preclinical reverse shoulder conditions using high-demand loading, relative to CoCr, and to assess counterface changes following intentional abrasive challenge.

Methods and Materials: Reverse shoulder wear testing was performed on a multi-station simulator using draft ISO/AWI 16436-2 guidance. 32-mm glenospheres (CoCr or ADLC-coated Ti6Al4V) were articulated against aged (ASTM F2003) UHMWPE humeral inserts manufactured from either conventional UHMWPE (25 kGy 1050) or vitamin E–stabilized highly crosslinked UHMWPE (150 kGy 1020-E). Testing included 5.0 million cycles (MC) of clean wear (Mode I) followed by intentional abrasive conditioning of glenospheres and an additional 5.0 MC of abrasive wear (Mode III) (total 10 MC). Gravimetric wear was measured at scheduled intervals, with surface roughness (white light interferometry) characterized at baseline, 5.0 MC, post-conditioning, and 10.0 MC. SEM/EDS was performed on representative glenospheres to characterize surface damage and coating/substrate exposure after conditioning and at 10.0 MC. Wear debris was characterized per ASTM F1877.

Results: Under clean conditions, both UHMWPE formulation wear rates were similar between CoCr and ADLC counterfaces. For conventional UHMWPE (25 kGy 1050), clean wear rates were 23.5 ± 6.6 mg/MC (CoCr) and 31.0 ± 17.1 mg/MC (ADLC); abrasive wear increased substantially for both counterfaces to 182.6 ± 22.0 mg/MC (CoCr) and 143.9 ± 100.7 mg/MC (ADLC). For vitamin E–stabilized highly crosslinked UHMWPE (150 kGy 1020E), clean wear rates were 2.4 ± 0.8 mg/MC (CoCr) and 3.1 ± 1.1 mg/MC (ADLC); after abrasive challenge, wear increased for CoCr to 6.6 ± 2.4 mg/MC but remained unchanged/decreased for ADLC to 2.6 ± 0.3 mg/MC.

CoCr glenospheres demonstrated measurable gravimetric wear under clean and abrasive conditions (e.g., 0.4 ± 0.2 mg/MC in clean testing for both studies; abrasive values remained measurable), while ADLC glenospheres demonstrated undetectable/near-zero wear rates (e.g., ~0.0 mg/MC; negative values indicating mass gain were reported under clean conditions in the 150 kGy study). Abrasive conditioning produced an immediate roughness increase for both counterfaces (order-of-magnitude increase), with initial scratch heights ~1 µm. After abrasive cycling to 10 MC, CoCr glenospheres showed continued roughening/scratch severity progression, whereas ADLC glenospheres showed a reduction in roughness from the post-conditioning state (surface stabilization). SEM findings were consistent with persistent multidirectional scratching on CoCr surfaces through 10 MC and limited progression of coating removal on ADLC surfaces from post-conditioning to 10 MC; EDS confirmed exposed titanium in abraded regions where coating was disrupted.

Particle size distributions for UHMWPE and ADLC debris were predominantly submicron across clean and abrasive conditions. Reported ECD distributions and summary metrics (mean/median) did not indicate emergence of a distinct larger-particle population attributable to abrasive challenge; particle morphologies were described as granular/flake-like for ADLC and spheroidal/granular for UHMWPE.

Discussion: Under high-demand reverse shoulder wear conditions with intentional third-body challenge, the proprietary ADLC-coated titanium counterface appeared to better preserve UHMWPE articulation after abrasion than CoCr. This effect was poly-formulation-dependent and most pronounced for vitamin E–stabilized highly crosslinked UHMWPE, where abrasive challenge increased wear against CoCr but not against ADLC, whereas conventional UHMWPE showed increased wear against both counterfaces. These findings suggest that the benefit of the ADLC counterface is not simply low counterface wear, but preservation of a more favorable articulating surface for polyethylene after surface insult. Supporting this interpretation, both counterfaces roughened immediately after conditioning, but CoCr continued to roughen during subsequent cycling while ADLC showed post-challenge surface stabilization, with SEM/EDS demonstrating localized coating disruption without evidence of progressive delamination through 10 MC. In addition, debris remained predominantly submicron across conditions without emergence of a distinct larger-particle population after abrasion. Collectively, these findings suggest that ADLC-coated titanium may help maintain polyethylene wear performance under adverse articulation conditions, particularly for advanced UHMWPE formulations.

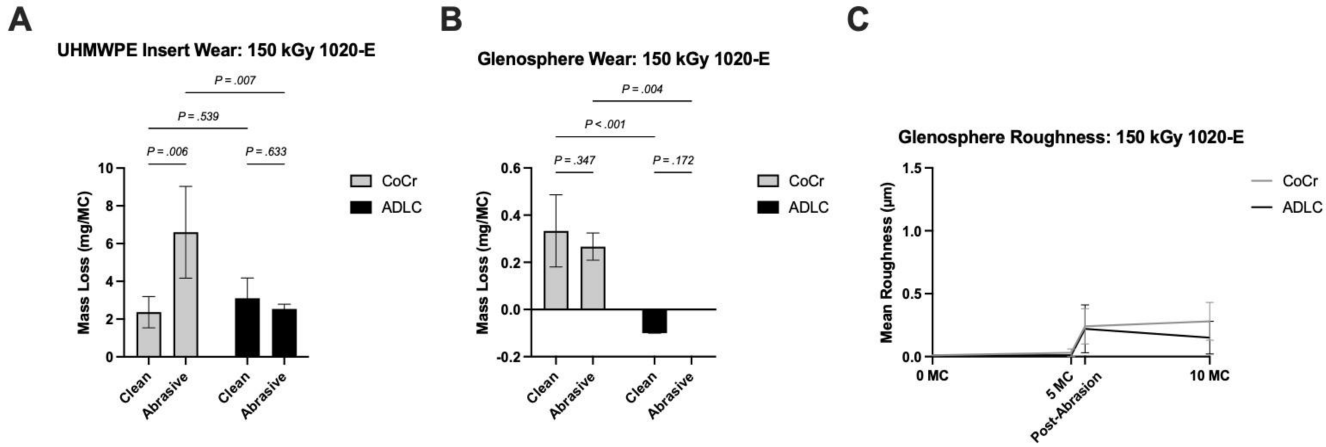

Figure 1. Wear and surface roughness outcomes for 150 kGy 1020-E UHMWPE articulated against CoCr or ADLC glenospheres under clean and abrasive conditions. (A) Mean ± SD UHMWPE humeral insert wear rates during clean (Mode I, 5 MC) and abrasive (Mode III, 10 MC) testing. **(B)** Mean ± SD glenosphere wear rates under clean and abrasive conditions. **(C)** Mean ± SD glenosphere surface roughness (Ra) at baseline (0 MC), post-abrasive conditioning, and 10 MC, showing divergence in counterface behavior after abrasion (CoCr roughening vs ADLC stabilization).

Polyethylene wear in combination with ceramic femoral components in total knee replacement under standard and abrasive conditions

Porporati, AA[1], Lackner, I[1], Gebert de Uhlenbrock, A[1]
[1]CeramTec GmbH, Plochingen, Germany
a.porporati@ceramtec.de

Introduction: To date, femoral and tibial components made of CoCr are the most commonly used in total knee arthroplasty (TKA). However, material-related complications discussed in the literature have increased interest in alternative materials on the market. As a result, TKA alternatives such as implant coatings and other materials are increasingly entering the market. Ceramics, particularly alumina matrix composites (AMC), represent an alternative material for TKA femoral and tibial components. Zirconia-toughened alumina ceramic components in TKA have been available on the market since 2006 as alternative for patients with metal hypersensitivity. A new ceramic TKA implant with an updated design has been granted Breakthrough Device Designation by FDA. This new metal-free ceramic TKA implant consists of a vitamin E-blended highly crosslinked UHMWPE tibial insert and BIOLOX®*delta* femoral and tibial components. The goal of the present study was to investigate the wear performance of a ceramic femoral and tibial component in combination with a polyethylene insert under standard and abrasive conditions using zirconium dioxide and PMMA particles.

Methods and Materials: An investigational ceramic TKA system, consisting of an AMC ceramic (BIOLOX®*delta*, CeramTec GmbH, Plochingen) femoral and tibial component, a polyethylene insert and patellar component, and the corresponding instrumentation for knee replacement surgery was investigated. The polyethylene used is a highly crosslinked UHMWPE (GUR 1020-E, 75kGy) blended with vitamin E at 1000 ppm (0.1%wt) with no temperature treatment after crosslinking and EtO sterilization. For the study, two different wear tests were performed. The standard wear test was conducted according to ISO 14243-1 for up to 5 million cycles. The abrasive wear test followed the same kinematic principle but included abrasive wear particles in the diluted calf serum and was conducted up to 3 million cycles. For the abrasive wear particles, a bimodal PMMA cement with zirconium dioxide slurry (particle sizes ~50 µm and ~500 µm) of 5g/l was used as lubrication medium. Prior testing, all inserts underwent aging according to ASTM F2003-02 for four weeks to assess the risk of polyethylene degradation during shelf life. Size and shape of the produced particles were determined for both tests and wear rate, oxidation index and surface roughness of the bearing surfaces prior and after testing were investigated.

Results: The wear rates of the standard and abrasive wear tests were 1.49 mg/Mc ± 0.07 mg/Mc and 24.47 mg/Mc ± 13.07 mg/Mc, respectively. The oxidation index before and after testing was below 0.1. After standard wear testing, the machine imprints were still visible on the insert, but the articulating surface was polished, decreasing the roughness from 1.17 µm to 0.08 µm. The roughness of the ceramic femoral and tibial components did not change.
After abrasive wear testing, the roughness Ra of the articulating surface of the insert increased to 3.29 µm in comparison to 1.12 µm prior testing. Pitting and scratching of the insert surface were observed. No scratching or matting was visible on the ceramic components. The average size of the polyethylene wear particles ranged from 0.28 µm to 0.40 µm in both tests.

Discussion: The goal of the present study was to investigate the wear generation of polyethylene in combination with a ceramic femoral and tibial TKA component under standard and abrasive conditions. Blending of the insert with vitamin E increased its resistance for oxidation and aging even in abrasive wear conditions. Typically, the wear rate for standard wear tests lies within a range from 5 mg/Mc to 30 mg/Mc[1]. Therefore, the measured wear rate of the insert in the present study with 1.49 mg/Mc ± 0.07 mg/Mc was very low. For the abrasive wear test, the increase in insert wear was 16-fold in comparison to the standard wear test, but still within the accepted range. The ceramic components did not show any signs of scratching. The shape, size and concentration of polyethylene wear debris is a critical factor in the longevity of knee arthroplasty. In the present study, particle characteristics did not differ between standard and abrasive wear conditions. The wear particles were smaller than those reported for conventional polyethylene, which may be attributed to crosslinking. In conclusion, polyethylene insert wear with ceramic femoral and tibial components was low under standard and within the acceptable range under abrasive conditions, with rates comparable to conventional polyethylene, offering an alternative in TKA.

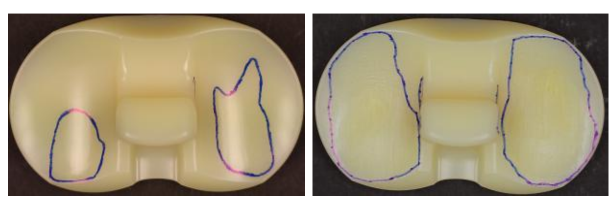

Figure 1: Surface of the insert after standard (left) and abrasive (right) wear testing.

References: [1]Grupp et al., 2013, *Journal of BiomechanicsDisclaimer:*

The investigated ceramic knee has been granted Breakthrough Device designation. This device is not cleared or approved by the FDA for distribution in the United States. The investigated ceramic knee is under development and is not approved by any regulatory authority or notified body. For product, safety, and risk information, always refer to the labelling of the legal manufacturer.

The oxidation resistance of UHMWPE containing a chemically bonded Vitamin E analog

Carvalho, BL[1]; Bellare, A[1]
[1]Polymerix Technologies, Boston, MA, USA *anuj@alum.mit.edu*

Introduction:
The post-gamma sterilization oxidative aging of ultra-high molecular weight polyethylene (UHMWPE) has historically been a major issue since it has been shown to affect the long-term clinical performance of joint replacements, and associated with delamination wear of tibial inserts of total knee replacements[1]and accelerated particulate wear in total hip replacements[2]. A common strategy to induce oxidative resistance to UHMWPE is to add a small weight percentage of synthetic Vitamin E[3] (alpha-tocopherol)(Figure 1(a)) or an alternative hindered phenol to the UHMWPE resin and to mold sheets or extrude rods from which implants are machined and sterilized. The antioxidant remains dispersed within the UHMWPE and free to quench free radicals that diffuse out of the lamellar phase into the amorphous phase where the antioxidant resides. While it has been shown that a larger than the historical 0.1% (by weight) Vitamin E (**VE**) is preferable for enhanced oxidation resistance[3], the amount is limited by the possibility of Vitamin E leaching out of the implant. In this study, we synthesized a Vitamin E analog capable of chemically bonding to UHMWPE by reacting 6-Hydroxy-2,5,7,8-tetramethylchroman-2carboxylic Acid (or Trolox)(**VET**) (Figure 1(b)), a water soluble Vitamin E derivative with 2-(3-methyl-3Hdiazirin-3-yl)ethan-1-ol (Diazirine alcohol) since diazirines have been shown to insert themselves into C-H, N-H and/or O-H bonds, the first of which is present in abundance in polyethylene with nitrogen gas as a reaction byproduct that can be easily vented off[4]. The resulting molecule, 2-(3-methyl-3H-diazirin-3-yl)ethyl-6-hydroxy2,5,7,8-tetramethyl chromane-2-carboxylate (or Troloxdiazirine ester)(**VED**)(Figure 2), was added to UHMWPE and oxidation resistance was evaluated using oxidation induction time (OIT).

Materials and Methods:
SYNTHESIS: Trolox (0.331 mmol) was dissolved in 10mL mixture of dichloromethane/acetonitrile (90:10 v/v), cooled to 0˚C. 0.361mmol carbonyldiimidazole was added followed by 1.0 equivalent diazirine alcohol and stirred overnight followed by purification of the product, which was subjected to proton nuclear magnetic resonance (NMR) to verify the structure.
COATING: A 12 mM solution of VE, VET or VED in acetone were added to 2g of GUR 1020 UHMWPE powder followed by continuous shaking and evacuation of the solvent until the powder was dry to provide identical 3 μmole antioxidant (0.1 wt% for VED) per g of UHMWPE. COMPRESSION MOLDING: Approximately 1g of the powder was added to a 2cm diameter, 0.3cm thick silicone mold followed by heating to 180˚C in a vacuum thermal press at 2 MPa applied pressure and then slow cooled after 30min at 180˚C.
OXIDATION INDUCTION TIME (OIT): A differential scanning calorimeter (DSC)(TA Instruments Q1000) was used to make OIT measurements using approximately 5mg of UHMWPE with no antioxidant (control), VE, VET and VED, respectively (n=3) using the method according to ASTM D3895. The procedure was to ramp to 200˚C at 10˚C/min in nitrogen gas, isothermal hold for 5min, isothermal hold for 90min using flowing oxygen and then cool to 40˚C at 20˚C/min.

Results: The OIT for the control UHMWPE containing no antioxidant was less than 1 min (Table 1), in agreement with a previous study[5]. All three VE, VET and VED containing UHMWPEs had substantially higher OITs with VE UHMWPE being the highest, VET having a 38% lower OIT and VED having a 31% lower OIT ($p<0.05$, ANOVA). It must be noted that all UHMWPEs had the same molar percentages of antioxidant while the weight percent of VED UHMWPE was 0.1%, VET UHMWPE was 0.075% and VE UHMWPE was 1.3%, respectively.

Discussion: This study showed that the presence of 3 μmol of antioxidant per 1g of UHMWPE increased the OIT substantially compared to UHMWPE control containing no antioxidant. The highest oxidation resistance was with Vitamin E, which is known to be a very stable and effective antioxidant. Trolox had the second highest oxidation resistance but lower than that of Vitamin E, likely due to its much higher hydrophilicity that makes it difficult to diffuse into the UHMWPE powder during molding so that it remains segregated at the interface. It is likely that the chemically bound diazirine functionalized Vitamin E had the lowest oxidation resistance since it is anchored to UHMWPE macromolecules and not mobile like Vitamin E or Trolox despite being less hydrophilic than Trolox. Nevertheless, addition of a higher weight percent of Vitamin E-diazirine could match the oxidation resistance of Vitamin E containing UHMWPE. Considering that it chemically binds to UHMWPE, there is also no likelihood of it leaching from the implant into peri-prosthetic tissue. Thus, if much higher oxidation resistance is desired, the diazirine functionalized Vitamin E can be safely added to UHMWPE without concerns of it leaching out. Furthermore, considering that diazirines are known to insert themselves into C-H, N-H or O-H bonds, it could be incorporated into the bulk or surfaces of a host of polymeric implants such as those comprising acrylic bone cement, poly(aryl ether ketones), silicones, resorbable synthetic polymers like polylactides, polyethylene oxide, and biological macromolecules such as alginates, collagen, silk and other proteins for tissue engineering applications.

References: (1) Bell et al, J Arthrop, 1998, 13(3), 280 (2) Besong AA et al, Biomed Mater Eng, 1997, 7(1), 59 (3) Xu et al, J Orthop Res, 2018, 36(7), 1860 (4) de Zwart et al, Science, 2019, 366 ,6467 (5) Muratoglu et al, J Orthop Res, 2024, 42:306.

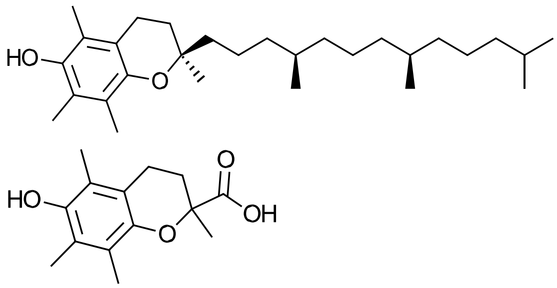

(a)

(b)

Figure 1. Molecular structure of (a) alpha-tocopherol and (b) Trolox

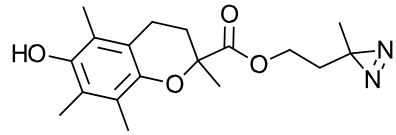

Figure 2. Molecular structure of diazirine functionalized Trolox.

Table 1. OIT (min) for control UHMWPE and UHMWPE containing 0.15mmol antioxidants (mean ± stdev).

Sample	OIT (min)
Control	<1
3□mol VE	40.9 ± 1.4
3□mol VET	25.4 ± 1.3
3□mol VED	15.8 ± 0.4

A Solution to Potentially Eliminate Oxidative Degradation and Enhance the Functional Performance of UHMWPE Liners in Artificial Joints.

Rizwan Mahmood Gul and Muhammad Kaleem Ullah Khalil
Department of Mechanical Engineering, University of Engineering and Technology, Peshawar, Pakistan
rgul@uetpeshawar.edu.pk

Introduction Ultra-high molecular weight polyethylene (UHMWPE) is the bearing material that is most commonly used in total joint replacement (TJRs) due to its biocompatibility and extensive clinical history. However, generation of wear particles and oxidative degradation reduces the longevity of implants. Wear debris starts osteolysis and aseptic loosening. Radiation crosslinking, is used to increase wear resistance, however, it produces residual free radicals, which remain in crystalline domains and promote long-term oxidation and embrittlement. Antioxidants are added to inhibit oxidative degradation. The only clinically approved stabilizer, vitamin E (VE) is a potent scavenger of radicals but has been shown to decrease crosslink density in high concentrations and fails to completely prevent oxidation in vivo. This results in the need to find alternative antioxidants which impart strong stabilization and have a minimal effect on network formation. This study assesses Quercetin (Q), a polyphenolic antioxidant with various hydroxyl functional groups, as a potential alternative to VE. UHMWPE with 0.5 wt% Q was compared with a similar VE blend. Quercetin is expected to provide better oxidative coverage and maintain the crosslink architecture due to its better hydrogen-donating ability.

Methods and Materials: Medical-grade UHMWPE (GUR 1050) was mixed with 0.5 wt%. VE and Q dissolved in isopropanol, vacuum dried, and then compression molded (200°C, 10 MPa). VE-UH and Q-UH signifies the produced blends. To crosslink, samples were electron-beam irradiated at 150 kGy. Oxidation induction time (OIT) was determined using the differential scanning calorimetry (DSC) at 200°C in the presence of oxygen. The crosslink density was determined through samples swelling in xylene using Flory theory.

Results: Control UHMWPE exhibited quick oxidation, while antioxidant blends delayed the oxidation (Figure 1). Figure 2 show that Q-UH yielded the highest OIT in both uncrosslinked and crosslinked conditions, extraordinarily higher than VE-UH. Irradiation reduced the OIT in all the specimens, but most significantly in VE-UH, while Q-UH remained capable of maintaining a high antioxidant activity. Crosslink density values were 226.2 mol/m³ (Control-UH), 196.9 mol/m³ (VE-UH) and 328.7 mol/m³ (Q-UH) (Figure 2). Quercetin, as compared to VE, did not inhibit network formation.

Discussion and Conclusions: Antioxidant chemistry has a noticeable effect on the performance of irradiated UHMWPE blends. VE minimized crosslink density by scavenging the radicals produced during irradiation, on the other hand, Quercetin retained rather increased network building and showed extraordinary oxidative resistance. The high crosslinked structure of Q-UH has the benefits of wear resistance and mechanical durability, both of which are required of orthopedic implants. Besides the crosslink density, the Oxidation Induction Time (OIT) findings also shed more light on the stabilizing performance of the various antioxidants. The significantly high OIT values obtained in uncrosslinked and irradiated versions of Q-UH indicate high resistance to oxidative degradation compared to VE-UH and Control-UH. Though irradiation decreased OIT of all blends due to the presence of entrapped free radicals, the decrease was greatest in VE-UH, indicating that vitamin E is less effective after the irradiation. Conversely, Q-UH exhibited significantly greater OIT following crosslinking indicating that Quercetin is an effective antioxidant even when subjected to radiation. This enhanced oxidation stability coupled with high density underlines the compound benefit of Quercetin in maintaining the prolonged stability of the irradiated UHMWPE for use in TJRs.

Quercetin thus is a potentially effective alternative stabilizer, providing better oxidation resistance and not inhibiting crosslinking but possibly improving the structural performance of crosslinked UHMWPE.

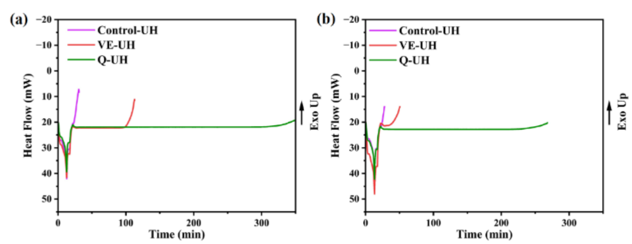

Figure 1: OIT DSC curves for (a) uncrosslinked and (b) crosslinked samples.

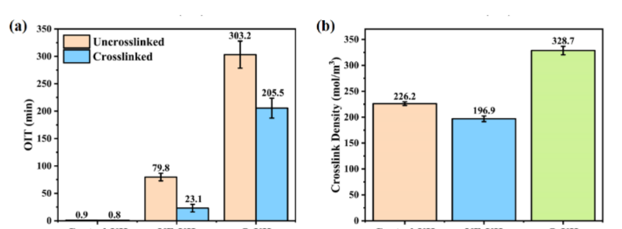

Figure 2: (a) OIT values of both uncrosslinked and crosslinked samples, and (b) their crosslink density

Free Radical Persistence and Oxidative Aging in Conventional and Vitamin E-Stabilized UHMWPE

Afsana Sharmin*[1], Farhan Azim[1], Benjamin M Walters[1] and M. Shah Jahan[1]

[1]Biomaterials Research Lab, Department of Physics and Materials Science, The University of Memphis, USA

asharmin@memphis.edu

Introduction: Ultra-high molecular weight polyethylene (UHMWPE) has been widely used as a bearing material in orthopedic implants since the 1960s due to its excellent mechanical properties and wear resistance. However, radiation sterilization can generate free radicals within the polymer structure, which may persist for long periods and initiate oxidative degradation. Understanding the long-term stability of radiation-induced radicals and the effectiveness of antioxidant stabilization is crucial for assessing the long-term performance and durability of implants. This study investigates the persistence of radiation-induced radicals in UHMWPE stored for 25 years under different environmental conditions, and examines the long-term free radical status of vitamin E-blended UHMWPE after 17 years of aging in air.

Materials and Methods: Conventional ultra-high molecular weight polyethylene (UHMWPE) samples stored for 25 years under different conditions (varying temperatures in air and vacuum) were analyzed to evaluate the persistence and decay behavior of longlived free radicals. In addition, vitamin E-stabilized UHMWPE samples aged in air for approximately 17 years were examined to assess the long-term status of residual radicals following antioxidant stabilization. All samples were subjected to 30 kGy gamma irradiation at room temperature prior to aging. Electron Spin Resonance (ESR) spectroscopy was employed to detect and quantify free radical species in all samples. Complementary physicochemical characterization techniques were used to assess oxidation and structural changes in the polymer after extended aging. This study focuses on independently characterizing the long-term radical content in each material system rather than performing a direct comparative analysis between conventional and vitamin E-stabilized UHMWPE.

Results: Electron Spin Resonance (ESR) analysis of conventional UHMWPE after long-term aging revealed the persistence of radiation-induced free radicals, with a gradual decline in radical concentration over time. Samples aged in air showed the formation of oxygen-related radical species, while vacuum-aged samples retained predominantly primary radiation-induced radicals. Increasing aging temperature promoted further radical decay, and no detectable radicals were observed under elevated temperature air-aging conditions, indicating advanced oxidative degradation. For vitamin E-blended UHMWPE aged in air, spectroscopic analyses confirmed the presence of α-tocopherol and its role in stabilizing the material. ESR results demonstrated a noticeable reduction in residual free radical concentration, with higher antioxidant content contributing to improved radical suppression. X-ray diffraction (XRD) confirmed the retention of the characteristic crystalline structure of UHMWPE after long-term aging. Fourier Transform Infrared (FTIR) analysis indicated progressive oxidation in conventional UHMWPE under prolonged exposure, whereas the presence of vitamin E mitigated oxidative changes. Overall, the results highlight the long-term evolution of free radicals in conventional UHMWPE under different environmental conditions and demonstrate the stabilizing effect of α-tocopherol in reducing residual radical content after extended aging.

Discussion: Radiation-induced free radicals persist in both conventional and vitamin E-stabilized UHMWPE even after decades of aging. In conventional UHMWPE, radicals are still detectable in air and vacuum, and their decay is affected by oxygen and temperature. In vitamin E-blended UHMWPE, αtocopherol effectively reduces the concentration of residual radicals but does not fully eliminate them, demonstrating that long-lived radicals can persist during extended storage. These findings highlight the remarkable stability of radiation-induced radicals in UHMWPE and underscore the importance of antioxidant stabilization in mitigating, though not completely preventing, oxidative processes. The persistence of radicals over such long periods has significant implications for predicting implant durability, optimizing sterilization and storage protocols, and guiding the design of next-generation radiation-resistant polymeric biomaterials for orthopedic applications.

Lipid Peroxidation and UHMWPE Co-Oxidation in Orthopedic Implants: Emerging Evidence and a Novel Oxidation Pathway Hypothesis

J. Poves[1*], V. Canales[2], J. Badiola[2], J.J. Mateo[3], J.J. Panisello[3], P. Bracco[4], F. Medel[1]
[1] Department of Mechanical Engineering-I3A, Universidad de Zaragoza, Zaragoza, Spain
[2] Orthopedic Surgery and Trauma Service, Hospital Royo Villanova, Zaragoza, Spain
[3] Orthopedic Surgery and Trauma Service, Hospital Universitario Miguel Servet, Zaragoza, Spain
[4]Department of Chemistry, University of Torino, via Pietro Giuria 7, 10125 Turin, Italy
*Corresponding author email: jpoves@unizar.es

Introduction: Reactive Oxygen Species (ROS) initiate oxidation in ultra-high molecular weight polyethylene (UHMWPE) prosthetic components, leading to mechanical degradation and poor clinical performance [1]. Moreover, literature studies have identified another oxidation pathway mediated by squalene (SQ), a lipid constituent of synovial fluid (SF), that exacerbates UHMWPE oxidation even in the absence of detectable free radicals [2]. Nevertheless, other oxidation mechanisms could play a role in the degradation of orthopedic polyethylene components.

Lipid peroxidation (LPO), triggered by injury, inflammation, and other pathological states, represents a critical mechanism. While LPO free radical intermediates have short-life, their aldehyde products exhibit greater stability, high reactivity, and ready diffusivity [3]. In this sense, previous studies have also confirmed aldehydes as major products of SQ oxidation [4-5].

We hypothesize the existence of an additional oxidation pathway wherein LPO might generate diffusible aldehydes from pathological SF constituents. These highly reactive species would penetrate UHMWPE, potentially amplifying oxidation along their diffusion gradient.

Methods and Materials: A total of 18 retrieved acetabular inserts (3 gamma-air, 4 gamma-inert , and 11 Ethylene Oxide sterilized), made of UHMWPE were collected from revision surgeries. Thin slices (~150 microns) were microtomed from the retrievals. Once marked, Fourier-Transform Infrared (FTIR) spectroscopy was performed on unextracted historical gamma sterilized samples at 100-µm intervals from the implant surface to obtain in-depth profiles. After that, historical PE slices were cyclo-hexane extracted for 8h and they were FTIR measured again. Regarding EtO-sterilized samples, they were measured only once, without cyclo-hexane extraction, since no radiation-induced oxidation was [1]
expected. [2]
FTIR spectra were processed by means of a custom developed software (INFRARED-PE) featuring a [3]
deconvolution module for carbonyl species analysis [6]. Thus, ASTM Oxidation Indices (OI), as well as the concentration of a variety of carbonylic species located at 1650-1800 cm^{-1} region were computed. Furthermore, it was attempted to detect and quantify the presence of [4]
squalene at 1668 cm^{-1} [7]. Once separated and quantified, the in-depth profiles of the predominant carbonylic species [5]
were adjusted to a Diffusion Fick's Law (DFL), according to equation 1, where M corresponds to total amount of diffusing species ($mmol/cm^3$), D to the diffusion constant (μm^2/year), x to depth (µm), t to length *in vivo* (years).

$$C(x,t) = \frac{M}{\sqrt{\pi D t}} exp\left(-\frac{x^2}{4Dt}\right) \text{ (eq. 1)}$$

Results: In all the retrievals, aldehydes were the most abundant SF-derived species with an average maximum concentration of 0.064 $mmol/cm^3$. Other species were absent, except for a slight contribution of carboxylic acids (Fig 1). The concentration of aldehydes with depth fit well to a DFL behavior, obtaining an average R^2 of 0.95. In addition, the diffusion constant, D, values obtained averaged 44,8 μm^2/year and it appeared to decrease with implantation time (Fig. 2). Regarding the presence of squalene, we detected a small contribution in some samples, namely 2 gamma-air, 2 gamma-inert and 3 EtO-sterilized retrievals. Moreover, we confirmed that the concentration of squalene with depth also followed a DFL behavior in those samples. Lastly, OI-depth and aldehydes concentration-depth profiles exhibited a similar trend (Fig. 3).

Discussion: The present results confirm aldehydes as the most abundant species coming from SF absorption into UHMWPE acetabular inserts. The predominance of aldehydes in SF is also supported by LPO literature, as well as by squalene-triggered oxidation studies [2-5]. Moreover, the similarity between OI depth profiles and aldehyde diffusion trends supports our hypothesis that aldehydes might trigger an alternative oxidation pathway upon diffusion. This mechanism may operate in addition to the ROS pathway and could be propelled by squalene acting as an oxidation potential carrier. Although squalene was absent in some samples, it remains unclear whether this reflects its absence in SF or its prior transformation into aldehydes . More research is needed to ascertain what compounds are present in the synovial fluid , as well as their potential effects on UHMWPE oxidation.

References:

[1] F. J. Medel et al. (2009), *J Bone Joint Surg*, 91, 4, 839–849.
[2] E. Oral et al. (2012), *J. Biomed. Mater. Res. B Appl. Biomater.*, 100B, 3, 742–751,
[3] F. Guéraud et al. (2010), *Free Radic. Res.*, 44, 10, 1098–1124.
[4] E. Naziri et al. (2014). *Eur. J. Lipid Sci. Technol*, 116(10), 1400–1411.
[5] Y. Yao et al. (2024). *Journal of Agricultural and Food Chemistry*, 72(28), 15755–15764.hjiu
[6] M. Salvalaggio et al. (2006) *Polym. Degrad. Stab.*, 91, 11, 2775–2785.
[7] H. Jin et al. (2013). *J. Mol. Struct*, 1032, 203–206.

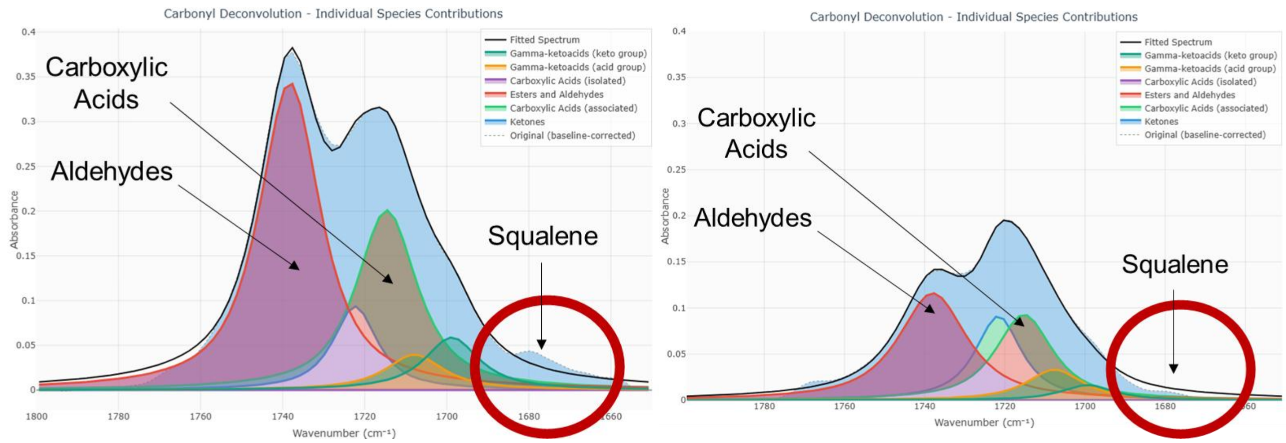

Fig 1. *FTIR Carbonyl peak (1650-1800 cm^{-1}) deconvolved, pre (left) and post (right) extraction from a gamma air irradiated UHMWPE retrieval, at 500µm depth, 19 years in vivo. Red circles highlight the presence (or absence) of squalene peak (1668 cm^{-1})*

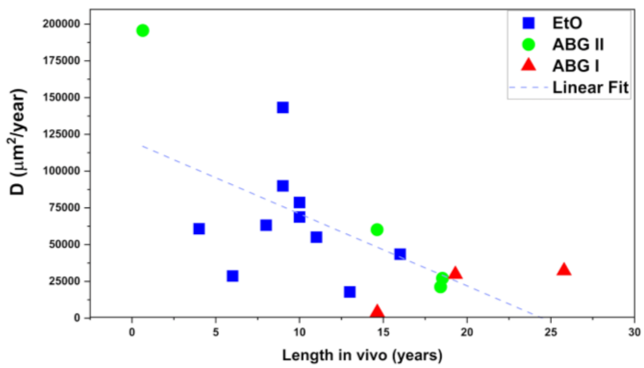

Fig 2. *Diffusion coefficient (D) versus length in vivo. Red triangles represent gamma air irradiated (ABG I), green circles gamma inert irradiated (ABG II) and blue squares ethylene oxide (EtO)-sterilized UHMWPE retrievals.*

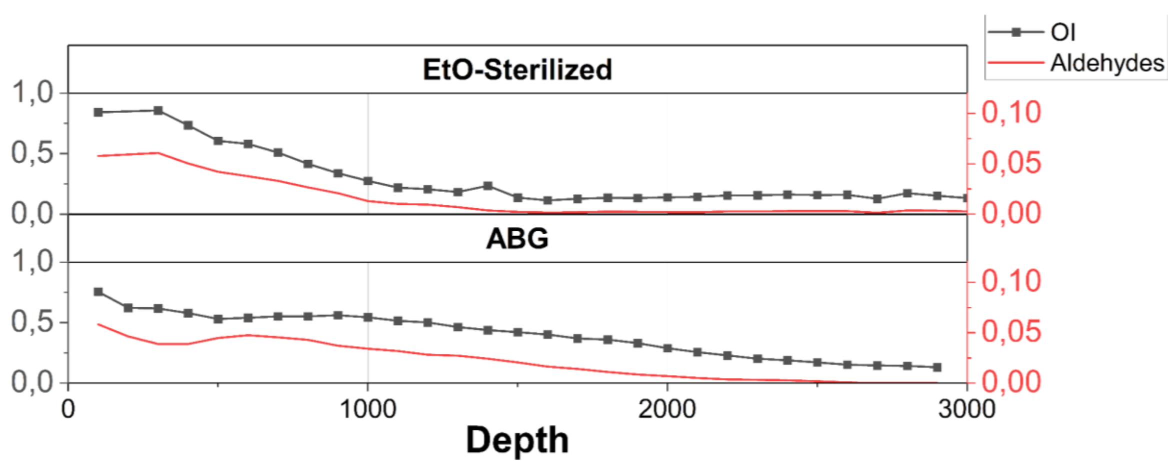

Fig 3. *Representative EtO-Sterilized (up) and gamma sterilized (down) retrievals oxidation indices and aldehydes concentration versus depth. OI was measured post-extraction.*

Failure of sequentially annealed highly cross-linked UHMWPE inserts – Is it related to oxidation?

T Bormann[1], S Van Onsem[2,3], SC Eiden[4], J Victor[5], C Van Der Straeten[6], E Blasco[3], JP Kretzer[1]

[1]Heidelberg University Hospital, Department of Orthopaedics, Research Center of Biomechanics and Implant Technology, Heidelberg, Germany. [2]Ghent University, Faculty of Medicine and Health Sciences, Ghent, Belgium. [3]AZ Alma, Department of Orthopedic Surgery, Eeklo, Belgium. [4]Heidelberg University, Institute for Molecular Systems Engineering and Advanced Materials, Heidelberg, Germany. [5]Ghent University, Department of Physical Medicine and Orthopaedic Surgery, Ghent, Belgium. [6]University Hospital Ghent, Health, innovation and research institute, Ghent, Belgium. *therese.bormann@med.uni-heidelberg.de*

Introduction:

Total joint arthroplasty for hips and knees is a successful treatment for degenerative joint diseases, which improves the quality of life of patients significantly. In total hip arthroplasty, the introduction of cross-linked polyethylene led to improved implant performance and longevity, because polyethylene wear is significantly reduced [1]. In total knee arthroplasty, the benefit of cross-linking is harder to judge. Polyethylene wear remains a failure reason in total knee replacement, and the evidence for improvement of implant performance is not as clear as in the hip [2]. Furthermore, different cross-linking strategies among the manufacturers may impact the wear behavior of the inserts. We present a case series of retrieved sequentially annealed highly cross-linked UHMWPE inserts that failed. Failure mostly occurred due to fracture in the posterior region of the inserts. Aside from fractures, some of the inserts showed visual signs of oxidation, such as subsurface whitening and delamination. The study aimed to clarify whether the observed failure mechanism of breaking posterior edges is related to oxidative degradation of the inserts.

Methods and Materials:

A series of 26 sequentially annealed failed inserts of one implant type was analyzed. Damage was investigated visually and rated by two observers using an established scoring method (Hood et al. [3]). Oxidation was measured on a subset of 12 inserts. The mean time in situ of the retrievals was 9.4 years ± 3.8 years (subset: 8.2 years ± 4.4 years). The retrievals were cut along the anterior-posterior direction through the condyle that exhibited the more severe damage. Slices of about 150 µm thickness were prepared from the specimens with a rotary microtome. Oxidation profiles of the ketone oxidation index (KOI) were measured by FTIR microscopy (Lumos-II, Bruker) in attenuated total reflectance mode in the posterior, middle and anterior region of the inserts. KOI was determined using the ketone peak height (1715 cm-1) normalized to the peak height of the 1368 cm-1 peak. Maximum KOI was used as measure for surface oxidation, while the bulk KOI was determined at about one millimeter length in the middle of each KOI profile. To assess the correlation between KOI, time in situ and damage score, Spearman's rank order correlation coefficient ρ was used. Statistical significance was set to $P < 0.05$.

Results:

Visual investigation of the inserts showed that 23/26 inserts exhibited fractures in the posterior region (Figure 1). 10/26 inserts exhibited subsurface whitening in regions other than the damaged posterior part. The mean Hood score was 58 ± 11 (range 39 – 80). On the subset, the average max. KOI was 1.8 ± 1.0. 9/12 inserts showed max. KOI > 1.3. The mean bulk KOI was 0.2 ± 0.1. Max. KOI increased with time in vivo (ρ=.84, P=.001). The Hood score, however, was not correlated to max KOI (ρ=-.13, P=.69) or bulk KOI (ρ=-.06, P=.86).

Discussion:

The sequentially annealed highly cross-linked inserts showed an increase in max. KOI with time in vivo. 66 % of the investigated inserts exhibited max KOI > 1.3, which indicates oxidative degradation that has the potential to deteriorate the mechanical properties of the inserts. The degree of damage, however, was not correlated to the degree of oxidation. Breakage of the posterior edge occurred in inserts that did not show elevated oxidation, too. Two of the inserts with max. KOI < 1 were of UHMWPE stabilized with antioxidants but nevertheless exhibited fractured posterior edges. On the other hand, two inserts exhibited max. KOI of > 3 but were not fractured. Further research is warranted to clarify what factors lead to the observed damage mechanism of breaking posterior edges. Also, the question remains whether the observed increase in oxidation is a general problem related to the specific cross-linking process of the inserts.

References:

[1] Kretzer et al., Orthopädie 50:2059-269, 2021.
[2] Asher et al., Arthroplast Today 30:101550, 2024.
[3] Hood et al., J Biomed Mater Res 17:829-842, 1983.

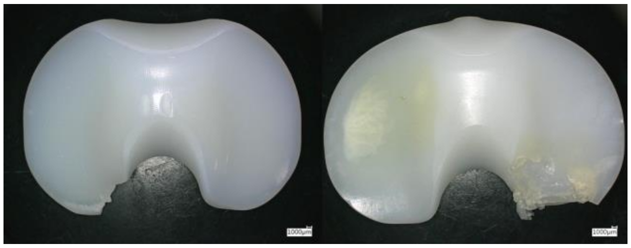

Figure 1: Inserts of the analyzed case series showing damage in the posterior region and subsurface whitening.

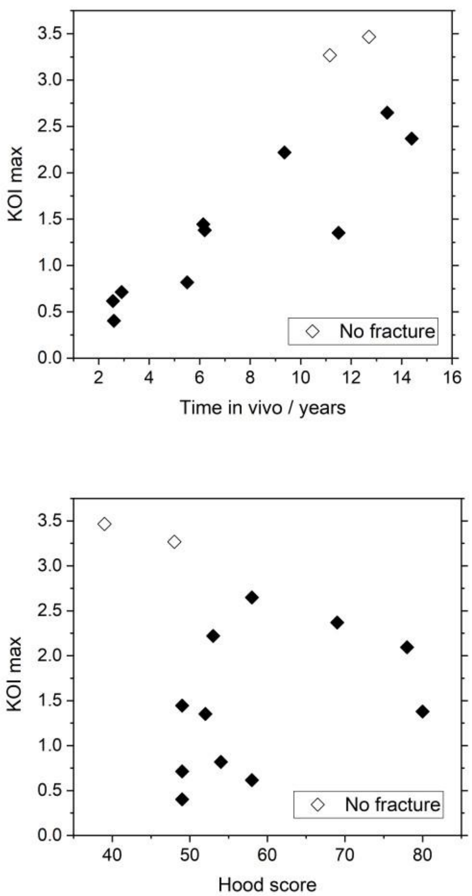

Figure 2: Max. KOI increases with time in vivo (top), but not with the degree of damage (bottom).

Oxidation Study of Super Crosslinked Gradient UHMWPE

Zongtao Zhang
b-ONE Ortho Corp, NJ
ZTZhang@b1.co

Introduction: Wear and toughness are usually compromised for bulk crosslinked UHMWPE. A super gradient crosslinked GUR1020-E (0.1wt% Vitamin E) has been made by UV assisted-chemical crosslinking [1]. It achieved super crosslinking (250 kGy) on bearing surface and low crosslinking (22 kGy) in the bulk material [2]. The material showed 3 times lower wear rate than 100 kGy crosslinked GUR1020-E in abrasive wear condition at 5 million cycles as well as high tensile strength 70 MPa and 422% elongation as conventional UHMWPE [3]. This study will further study the material oxidation resistance in O2 and air.

Material and Method: The standard 36J liners with thickness 8 mm and 8 mm thick flat plates were made by the super crosslinked gradient GUR1020-E (0.1wt% Vitamin E) by B-ONE Ortho Corp using UV assisted-chemical crosslinking method [3]. In this method, the sterilization is 25-40 kGy gamma ray in N2 protected aluminum coated polymeric pouch packaging. A post stabilization of free-radicals is conducted at 50ºC for 144 hours with the sealed packaging. The package 36J liners were opened and exposed the material in 5 atm O2 for 14 days at 70ºC per ASTM F2003-02. The liners at 45º from dome were cut and microtome into 200 µm film and measured oxidation index per ASTM F 2012-17 by Cambridge Polymers INC. The 8 mm thick flat plates were subjected to more seer oxidation than ASTM F2003-02 in convection oven at 100ºC in air for 14 and 28 days. The top super-crosslinked 0.25 mm layer of the plates were machined off from the plates and conducted small punch tests. The commercial highly crosslinked Stryker-X3 and B-ONE Ortho Corp's VE-PE (GUR1020-E,100 kGy) are oxidized in the same batch as in the same air convection oven. ions. Five samples were tested for each data point for the small punch.

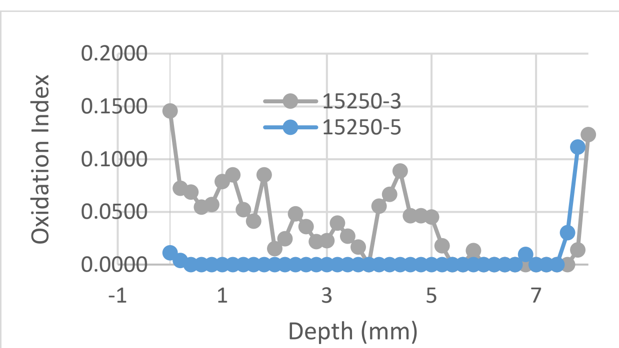

Figure 1. Oxidation indices super-crosslinked gradient GUR1020E (Sapphire GXL) acetabular liners. Samples 15250-5 was stabilized and not aged. Sample 15250-3 was stabilized and aged at 70ºC for 14 days in O_2 at 5 atm.

Results: Before 70ºC in O2 for 14 days aging (sample 15250-5), an extremely low oxidation index (0.01) on super-crosslinked bearing surface (250 kGy) and entire bulk material. A little high oxidation index of 0.12 at the backside of the liner at low degree of crosslinking (22 kGy). After 70ºC in O2 for 14 days aging (sample 15250-3), the low crosslinked backside (25-40 kGy) has the almost same oxidation index (0.13) as before aging, while super-crosslinked bearing surface gets a higher oxidation index of 0.15. The bulk material has a variable oxidation index below 0.10. At more sever oxidation in air at 100ºCs, the super-crosslinked bearing surface maintains the highest level of ultimate load, displacement, and work to failure at 0. 14, and 28 days of aging as compared to the commercial VE-PE (GUR1020-E,100 kGy) and Stryker-X3. The highest levels of small punch properties are attributed to its super-crosslinking (250 kGy). The little drop of small punch properties against aging time is attributed to Vitamin E protection. Stryker-X3 is the highly crosslinked UHMWPE without Vitamin E, it experienced a dramatic drop of small punch properties after 14 and 28 days at 100ºC in air.

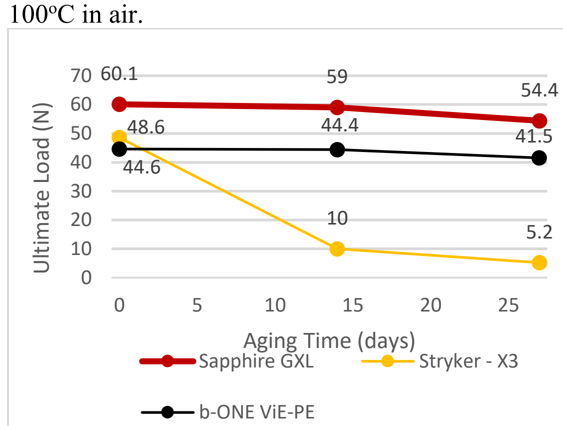

Fig.2. Ultimate load of small punch for Super-crosslinked GUR1020-E (Sapphire GXL) oxidized in air at 100ºC.

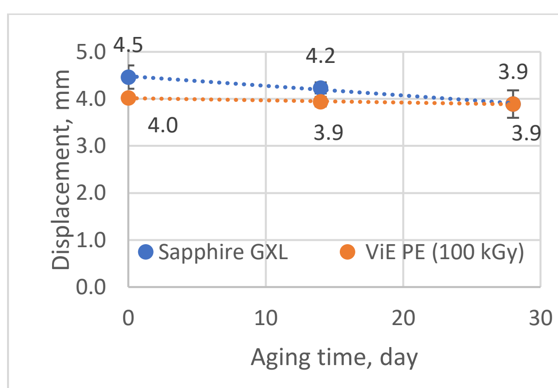

Fig.3. displacement of small punch for Super-crosslinked GUR1020-E (Sapphire GXL) oxidized in air at 100ºC.

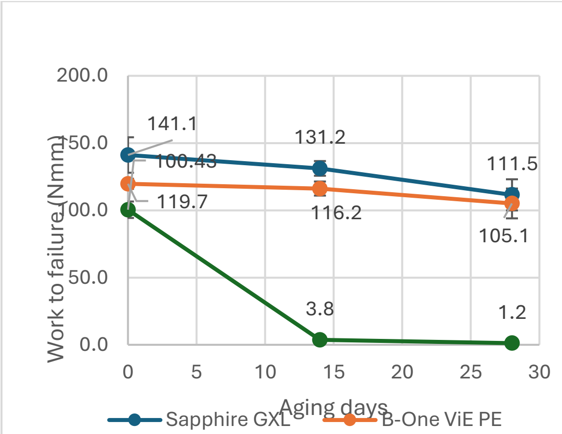

Fig.3. Work to failure of small punch for Super-crosslinked GUR1020-E (Sapphire GXL) oxidized in air at 100ºC.

Discussion: The super gradient crosslinked GUR1020-E has the best antioxidation resistance than the commercial highly crosslinked UHMWPE. Very high equivalent crosslinking degree (250 kGy) gives the material higher absolute values of ultimate load, displacement, and work to failure. The 0.1% vitamin E allows the material to maintain its stability with little degradation in the more challenging condition than ASTM F-2003-02 condition.

References: [1] Zongtao Zhang, US patent application 2022/0002452 (2022). [2] Nolan Lacombe, 2023 ORS Paper No.1207. [3] Zongtao Zhang, 2023 ORS Paper No.1643. [4] Zongtao Zhang, 2023 ORS Paper No.1208. [5] Hout, J. Caitlin et al, J. Biomed. Mat. Res, Part B, Vol 97, 2 (2011):327-33. [6] Harry A. McKellop, et al, J. Orthopedic Res., Vol.17, No.2 (1999):157-167. [7] King, R et al, 55th ORS meeting, Paper No.19.

Wear properties of bupivacaine/UHMWPE blends

Inverardi, N[1,2], Suhardi, VJ[1,2], Serafim, MF[1], Muratoglu, O[1,2], Oral, E[1,2]
[1]Harris Orthopaedics Laboratory, Massachusetts General Hospital, Boston, MA 02114
[2]Department of Orthopaedic Surgery, Harvard Medical School, Boston, MA 02114
eoral@mgh.harvard.edu

Introduction: Ultrahigh molecular weight polyethylene (UHMWPE) has been widely used as a bearing material in orthopaedic joint replacements. To further improve long-term implant performance, crosslinked UHMWPE has been developed to enhance wear resistance. For conventional and non-crosslinked UHMWPE articulating against metallic or ceramic counterfaces, wear behavior is primarily governed by asperity contacts and large-scale deformation of the polymer rather than by friction or lubrication conditions. Recently, drug-UHMWPE composites have emerged as multifunctional materials capable of delivering therapeutics locally to address clinical challenges such as post-operative pain and infection. These materials are typically produced by compression molding, which results in a phase-separated morphology where drug-rich domains are dispersed within the polymer matrix. Following drug release, these domains form a porous network whose structure depends on the size, spatial distribution, and connectivity of the initial drug phase. In this work, we investigated the combined influence of morphology-induced porosity and ionizing irradiation on the wear behavior of bupivacaine-loaded UHMWPE.

Methods and Materials: Bupivacaine hydrochloride was mechanically blended with UHMWPE at loadings ranging from 2 to 20 wt.%. Prior to blending, the drug was sieved through a 75 µm mesh and the sieved fraction only was used for incorporation into UHMWPE. The blends were compression molded at 170 °C under 20 MPa for 10 min, followed by cooling under the same pressure for at least 45 min. A subset of molded blocks was vacuum packaged in inert atmosphere and subjected to gamma irradiation at doses ranging from 0 to 75 kGy. The morphology of the cross-section of the consolidated material was observed by scanning electron microscopy (Zeiss Supra55VP FESEM, 2-5 kV) after sputter coating. The distribution and interconnectivity of drug domains and the resulting porous structure was evaluated after drug extraction obtained by elution in de-ionized water for 1 month at 37 °C. Cylindrical pin-on-disk specimens (diameter 9mm; height 13mm) were wear tested using a custom wear testing system (OrthoPOD). Samples were articulated against polished CoCr disks under a rectangular pattern (5x10 mm^2) at 2 Hz in undiluted preserved bovine serum. Wear rates were determined by linear regression of specimen mass loss as a function of the number of cycles between 0.5 and 1.128 million cycles.

Results: Compression molded drug-UHMWPE blends exhibited a phase-separated morphology, with dispersed and isolated drug domains at low drug loadings. Increasing drug loading promoted greater interconnectivity between domains, eventually forming a percolated structure that generated an interconnected porous network following drug elution (at drug loadings of 10-20 wt.%). The wear rate for porous and percolated UHMWPE (drug loading of 20 wt.%) was 6 mg/MC, approximately, while the wear rate for virgin UHMWPE was 14 mg/MC, approximately. In addition, the wear rate of virgin UHMWPE decreased linearly with increasing irradiation dose between 0 and 75 kGy ($R^2 = 0.97$). A similar linear decrease in wear rate with irradiation dose was also observed for porous UHMWPE ($R^2 = 0.92$), with wear rates consistently lower than those of irradiated virgin UHMWPE at every dose level. For porous materials, wear rates decreased from approximately 6 mg/MC at 0 kGy to approximately 2 mg/MC at 75 kGy.

Discussion: These findings suggest that the porous morphology generated by the drug domains before and after elution could act as an additional mechanism contributing to wear behavior in UHMWPE, independent of crosslinking. The wear rate for the porous and percolated material (~6 mg/MC at drug loading of 20 wt.%, 0 kGy) was substantially lower than that of non-crosslinked UHMWPE without drug additives and approached the wear rate of moderately crosslinked UHMWPE (~7 mg/MC at 50 kGy). When the porous and percolated material is subjected to the highest irradiation dose (75 kGy), there is a further reduction in wear rate (2 mg/MC) indicating that morphology-enabled wear resistance may be combined with conventional irradiation-induced crosslinking strategies to further improve the tribological performance of UHMWPE surfaces. It is important to note that this morphology-mediated wear reduction was observed for the case of the blends reported in this work and may not generalize to different drug/UHMWPE blends, as the discriminating factors that govern this behavior remain unclear. A deeper theoretical understanding of the mechanisms driving morphology-mediated wear reduction could enable the design of tailored porous microstructures that maximize wear resistance while ensuring that mechanical properties remain sufficient to maintain structural strength for load-bearing applications. Further, additional experimental studies would be valuable to clarify the role of the lubricating medium and its interaction with porous structures during articulation.

Acknowledgements: This work was supported in part by the Office of the Assistant Secretary of Defense for Health Affairs, through the Peer Reviewed Medical Research Program under Award No. W81XWH-17-1-0614 and in part by the Muratoglu-Harris Endowment.

Annealing's Impact on the Microstructure and Mechanical Behavior of Vitamin E Containing Highly Crosslinked UHMWPE

Daniel Weller[1], Brinda Badwe[1]
[1]Stryker Orthopaedics, Mahwah, NJ
Daniel.weller@stryker.com

Introduction: Post-irradiation thermal treatment of highly crosslinked UHMWPE has historically been required in the medical device industry to prevent gross oxidation and early failure. Significant research has been performed comparing the two types of thermal treatments, annealing and remelting, however little research exists comparing annealed to as-irradiated material. The common belief is that annealing preserves the as-annealed morphology and therefore mechanical performance is unchanged. This belief is broadly true when compared to the extreme changes remelting induces but misses that annealing also significantly changes morphology and performance. Newer, antioxidant containing UHMWPWEs, don't require thermal treatments like traditional formulations and today both as-irradiated and annealed formulations exist on the market. This raises the question, should antioxidant containing highly crosslinked UHMWPE be annealed post irradiation? This research analyzes the morphological and mechanical changes induced by annealing and explores the merits of its use in Vitamin E UHMPWEs.

.

Methods and Materials: Vitamin E containing UHMWPE bars were irradiated to 130 kGy and compared to analogs annealed at 120, 130, 135, and 150 °C. All samples were manufactured from a single bar of VE-UHMWPE (0.1 wt% VE 1020 GUR resin). Differential Scanning Calorimetry (DSC): was performed at 10°C/min between 40 and 200°C (n=3). Percent crystallinity was calculated by dividing the enthalpy of fusion by that of a fully crystalline UHMWPE (289.3 J/g). Swell Ratio Testing: was performed based on the procedures in ASTM D2765 (n=3) and crosslink density was calculated from the equation and parameters described in ASTM F2214. Small Punch Testing: was performed following ASTM F2977 (n=6). Double-Notched Izod Testing: was performed following ASTM F648 A1 (n=6). Pin-on-Disk Wear Testing: was performed on a three-station tester (Paltro, Unitest-550) n=3 following ASTM F732.

Results: Test results can be found in Table 1. We found that Annealed samples were stronger, more ductile, more crosslinked, and less impact resistant compared to as-irradiated samples. The exact effect of annealing was dependent on annealing temperature but at all annealing temperatures max load was increased by more than 16% and displacement at break increased by more than 25% (Figure 1). As annealing temperature increased more partial melting occurred reducing the materials crystallinity. The less crystalline material showed further increases in max load and displacement, increased fracture toughness, and decreased yield. Annealing at all temperatures significantly increased crosslink density (>22%) but didn't have a measurable effect on material wear (pin-on-disk). Crosslink density differences of this magnitude should have observable differences in wear. This suggests that when using crosslink density to predict wear properties it is critical to consider the materials thermal history, as annealing may raise crosslink density without affecting wear.

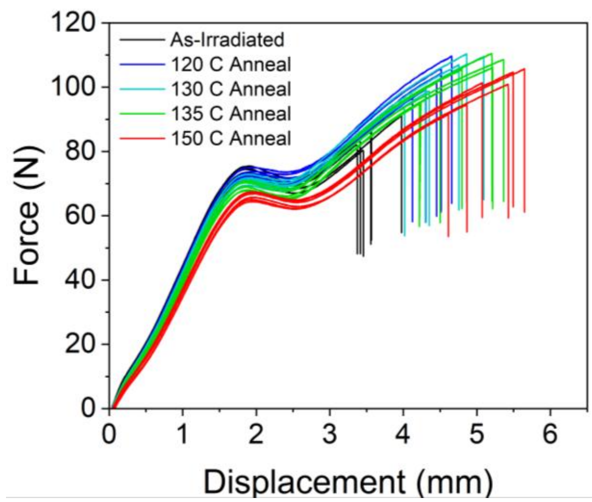

Figure 1. Small Punch mechanical data at various annealing temperatures

Discussion: With the introduction of antioxidants such as Vitamin E to UHMWPE, post irradiation thermal treatment has become optional for oxidative resistance. It is therefore prudent to understand how annealing impacts mechanical performance so manufacturers can make informed decisions on how to process their material. Annealing appears to have a net positive influence on mechanical performance improving both strength and ductility, however impact strength was reduced. It's possible there is an application in which low wear and high impact strength are the critical parameters in which case an as-irradiated part may make sense, however the loss in impact strength from annealing (<10%) is minimal and becomes even less significant at high annealing temperatures. Based on the tests performed in this study, there appears to be significant mechanical benefit to annealing highly crosslinked vitamin E UHMWPE. Optimal annealing occurred between 120 and 130°C with the lower temperature anneal offering better yield strength and the higher temperature anneal offering higher impact strength. Annealing at any temperature significantly increased strength, ductility, and crosslink density but did not impact wear rates. Further testing evaluating device performance is needed to confirm these results.

Table 1: Results summary of vitamin E highly crosslinked UHMWPE annealed at different temperatures

Annealing Temp			None	120 °C	130 °C	135 °C	150 °C
Small Punch	Max Load (N)	*avg*	85.3	102.4	102.9	103.0	99.2
		stdev	4.0	4.8	7.0	5.5	6.1
	Max Disp. (mm)	*avg*	3.5	4.4	4.5	4.5	5.2
		stdev	0.2	0.2	0.4	0.5	0.4
	Yield Load (N)	*avg*	73.6	73.1	71.2	69.2	66.1
		stdev	1.6	1.2	1.2	1.2	2.0
Izod	W (KJ / m2)	*avg*	63.0	57.4	61.1	62.9	68.7
		stdev	2.2	1.2	1.3	1.5	0.6
DSC	Crystallinity (%)	*avg*	57.5	59.4	59.2	55.7	47.7
		stdev	0.1	0.6	0.6	0.2	1.5
Crosslink Density	(mol / dm3)	*avg*	0.106	0.130	0.133	0.137	0.139
		stdev	0.001	0.001	0.001	0.001	0.002
Wear	(mm3 / mc)	*avg*	3.34	3.60	na	3.33	na
		stdev	0.43	0.40	na	0.23	na

A Novel Method for Measuring Residual Stress in Consolidated Implantable Grade UHMWPE

Schindler, KM[1]
[1]Mitsubishi Chemical Group, Fort Wayne, IN, USA
katie.schindler@mcgc.com

Introduction: Residual stresses in implantable grade UHMWPE influence a variety of factors including dimensional stability. Quantifying residual stresses are challenging due to the material's viscoelasticity, semicrystalline structure and sensitivity to conventional stress-relief measures. Annealing of UHMWPE has traditionally been used to relieve internal stress following consolidation of the polymer.

In this work, we present a novel method for measuring residual stress in implantable grade UHMWPE which is minimally destructive. This approach leverages strain recovery to infer residual stress in unannealed versus annealed UHMWPE of various material types, shapes and annealing conditions.

Methods and Materials: Three types of implantable grade polymers were consolidated by ram extrusion. Samples were either left unannealed, specialty annealed, or standard annealed. A ¼" wafer was sliced from the extruded barstock and then a notch was machined into the wafer. Machining parameters were controlled for each group. Angle differences of notched UHMWPE were measured using a Keyence digital microscope.

Ten unannealed samples were prepared from a single batch of UHMWPE. Ten annealed samples were also prepared from the same batch of UHMWPE. Specimens were fabricated using controlled machining parameters. This process was repeated for three material sizes (**Table 1**). Samples were marked in controlled locations (**Figure 1**). Three operators were used to measure the notch angles and each operator measured each specimen twice. Minitab was used for statistical analysis.

Table 1: Summary of Materials and Annealing Conditions

Material	Shape	Annealing Conditions
GUR1020 custom blended	Small Rod	Unannealed / Standard Annealed
GUR1020	Profile	Unannealed / Specialty Annealed
GUR1050	Large Rod	Unannealed / Standard Annealed

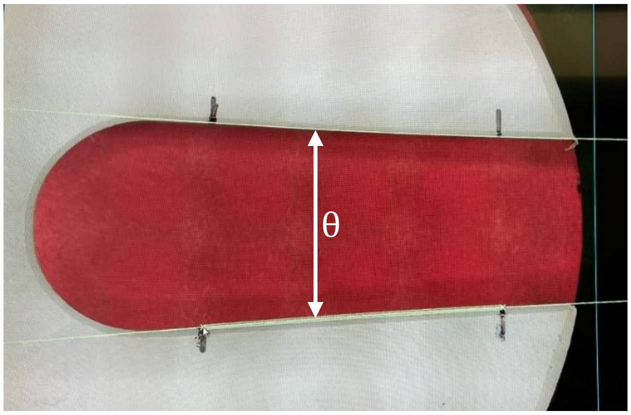

Figure 1. – Notch Angle Measurement Example

Results: Average notch angles of unannealed samples were higher compared to standard annealed and specialty annealed samples for each material type (**Figure 2**). Minitab Gage R&R XBar/R Method Results showed Total Gage R&R % Contribution was 2.39, Total Gage R&R % Study Variation was 15.47 and Number of Distinct Categories was 9.

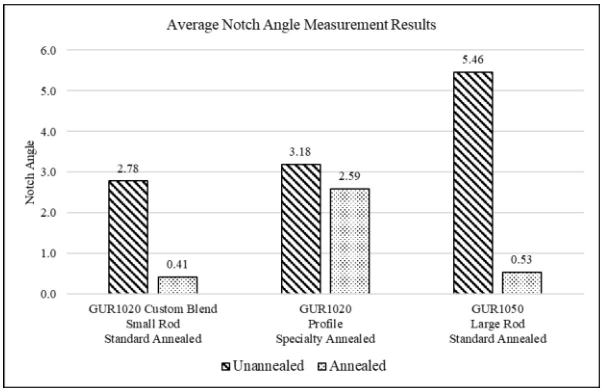

Figure 2. – Average Notch Angle Measurement Results

Discussion: This data shows promising results as a new test method for inferring residual stresses in consolidated implantable grade UHMWPE. The test method can also be used to compare existing annealing profiles with new annealing profiles in development. Further work could be performed assessing notch angles of these materials after irradiation and quenching. Additionally, this method could be investigated for a production environment to monitor annealing cycles over time.

Thickness-Driven Normalization of UHMWPE Small Punch Test Results for Expanded ASTM F2977 Usability

Tartaglia, Michael[1]; Aponte, Carlos[1]; Badwe, Brinda[1]
[1]Stryker Orthopaedics, Mahwah, New Jersey
michael.tartaglia@stryker.com

Introduction: Small punch testing has been widely adopted as a miniature-specimen method capable of capturing strength and toughness effects in ultra high molecular weight polyethylene (UHMWPE), particularly when only limited material is available – such as in retrievals. ASTM F2977 formalized this approach, although its tight dimensional tolerance for thickness poses practical machining and manufacturing challenges for many labs and machinists, resulting in high scrap rates, expensive machining costs, and unrealistic machining capabilities. Earlier work demonstrated clear scaling relationships between UHMWPE specimen thickness and small punch testing properties, including for load and displacement; that study focused on the intrinsic relationship of these properties as a relation to thickness range of 0.250mm to 0.500mm with fixture changes at each thickness level – suggesting that reliable normalization formulas could be derived to use samples that fall outside of the ASTM F2977 range [1]. Despite this earlier study, a gap remains regarding whether labs can systemically relax thickness tolerance requirements while preserving the comparability of small punch testing results. The current study presented here addresses that gap by quantifying thickness-dependent effects on small punch load-displacement behavior and establishing practical thickness-normalization formulas for broader usability of ASTM F2977 across the industry.

Methods and Materials: Small punch test coupons were prepared from sequentially crosslinked (90 kGy) and annealed (SXL) GUR1020 UHMWPE and Virgin GUR1020 UHMWPE, at nominal thicknesses of 0.500mm, 0.525mm, 0.550mm, and 0.575mm. Each coupon was machined to the ASTM F2977 tolerance of +0.013mm / -0.000mm, while keeping all remaining dimensions in conformance with ASTM F2977. Testing was performed using an Instron 5900 test frame and Bluehill Universal software. All test conditions and fixtures were maintained as prescribed in ASTM F2977 [2]. Data analysis was conducted in Microsoft Excel (for formula development and graphical outputs) and Minitab 21 (for one-way ANOVA).

Results: Changes in the small punch load-displacement response were observed as specimen thickness varied (Table 1, Table 2, Figure 1). In general, ultimate load increased and ultimate displacement decreased with increasing thickness. These trends were well described by power law relationships, yielding the following exponents: 0.84 for SXL ultimate load (r^2=0.95), -0.99 for SXL ultimate displacement (r^2=0.94), 0.87 for Virgin ultimate load (r^2=0.98), and -0.81 for Virgin ultimate displacement (r^2=0.83); no consistent thickness relationship was observed for work to failure, which remained relatively constant across the thickness range tested. Original load and displacement data were normalized using the power law transformation shown in Formula 1 (Table 3, Table 4, Figure 2); for simplicity and consistency, the exponents derived from the SXL group were applied to both material groups. Subsequent statistical analysis demonstrated that normalization substantially improved data comparability. One-way ANOVA test with Tukey pairwise comparison revealed no significant differences in normalized ultimate load (SXL: p=0.596; Virgin: p=0.982) or normalized ultimate displacement (SXL: p=0.587; Virgin: p=0.878). In contrast, the original (non-normalized) SXL data showed significant differences across thickness groups for both ultimate load and ultimate displacement (p=0.000 for both). Although the original Virgin data did not reach statistical significance for both ultimate load and ultimate displacement, the p-values (p=0.228 and p=0.042, respectively) reflected the same underlying thickness-related trends observed in the SXL group, with potentially more power needed to detect any differences. Work to Failure values demonstrated no statistical differences across thickness groups for either material (SXL: p=0.880; Virgin: p=0.999); recalculated values via normalization of the curve can be found in Tables 3 and 4 (SXL: p=0.908; Virgin: p=0.971).

Discussion: The findings of this study reinforce and extend prior work on UHMWPE small punch thickness effects, which established that power law normalization of load-displacement can reliably compare samples of differing thicknesses. The strong agreement between power law exponents across the two material groups, and with previous literature, supports the conclusion that small punch properties of UHMWPE are material intrinsic and not specific solely to the test fixture and conditions. By validating a reliable thickness normalization equation, this study provides a practical pathway for labs to broaden acceptable specimen thickness range, reducing scrap, minimizing the need for specialized machining, and enable flexibility with this test method. Further work is necessary to determine whether the same exponent values apply across broader UHMWPE material conditions, such as in an expanded study or in a round robin across multiple labs. If validated successfully, this approach may warrant consideration for inclusion as an alternative approach in ASTM F2977.

References:

[1] Kurtz et al *The Effect of Specimen Thickness on the Mechanical Behavior of UHMWPE Characterized by the Small Punch Test*. 2004.
[2] ASTM F2977.

Table 1. Summary of SXL small punch test results prior to power law normalization by thickness (mean ± stdev)

Specimen thickness (mm)	*Ultimate load (N)*	*Ultimate displacement (mm)*	*Work to failure (mJ)*
0.500	97.1 ± 3.7	4.3 ± 0.2	263.1 ± 19.0
0.525	103.4 ± 2.4	4.0 ± 0.1	256.0 ± 10.2
0.550	106.6 ± 2.9	3.9 ± 0.2	261.7 ± 18.2
0.575	109.2 ± 1.8	3.7 ± 0.1	257.3 ± 5.7

Table 2. Summary of Virgin small punch test results prior to power law normalization by thickness (mean ± stdev)

Specimen thickness (mm)	*Ultimate load (N)*	*Ultimate displacement (mm)*	*Work to failure (mJ)*
0.500	56.4 ± 3.5	4.8 ± 0.1	248.6 ± 12.5
0.525	58.7 ± 1.2	4.5 ± 0.1	249.5 ± 6.4
0.550	60.9 ± 2.7	4.4 ± 0.0	250.5 ± 2.7
0.575	64.3 ± 5.3	4.1 ± 0.3	250.1 ± 26.7

Table 3. Summary of SXL small punch test results after power law normalization by thickness (mean ± stdev)

Specimen thickness (mm)	*Ultimate load (N)*	*Ultimate displacement (mm)*	*Work to failure (mJ)*
0.500	96.6 ± 3.7	4.3 ± 0.2	263.4 ± 19.0
0.525	99.0 ± 2.2	4.2 ± 0.1	258.0 ± 10.3
0.550	97.9 ± 2.6	4.3 ± 0.2	265.7 ± 18.5
0.575	96.9 ± 1.5	4.3 ± 0.1	262.8 ± 5.9

Table 4. Summary of Virgin small punch test results after power law normalization by thickness (mean ± stdev)

Specimen thickness (mm)	*Ultimate load (N)*	*Ultimate displacement (mm)*	*Work to failure (mJ)*
0.500	55.9 ± 3.5	4.6 ± 0.3	248.9 ± 12.5
0.525	56.1 ± 1.2	4.8 ± 0.1	251.5 ± 6.4
0.550	55.9 ± 2.5	4.9 ± 0.1	254.4 ± 2.7
0.575	56.9 ± 4.6	4.7 ± 0.4	255.6 ± 27.4

Formula 1. Thickness normalization calculation

$$\gamma_{0.500} = \gamma_0 \times \left(\frac{0.500}{t_0}\right)^n$$

where, γ_0 is the original data point, t_0 is the original sample thickness, and n is the exponent (0.84 for load; -0.99 for displacement)

Figure 1. Representative small punch original load-displacement curve for SXL group as a function of thickness

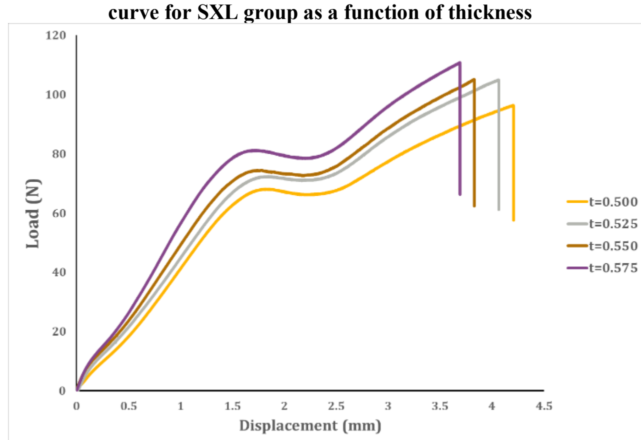

Figure 2. Representative small punch normalized load-displacement curve for SXL group as a function of thickness

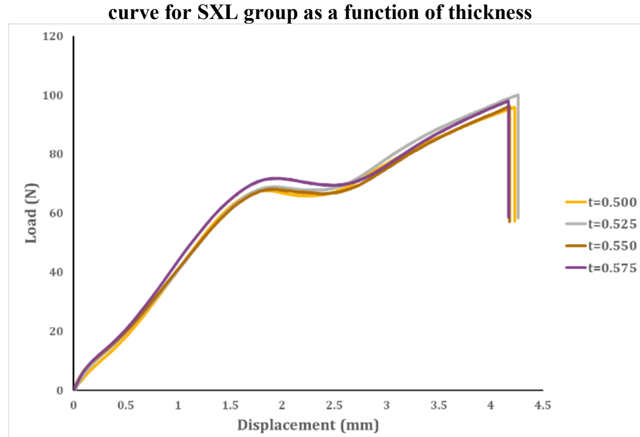

Gentamicin-Eluting UHMWPE as a Durable, Antimicrobial Spacer Material for Two-Stage Revision Arthroplasty

Mehmet D. Asik, PhD[1,2], Timothy Zhao, BA[1], Olivia Geitz, BS[1], Matheus Ferriara, BS[1], Lucy C. Bowden, PhD[1,2], Keith K. Wannomae, BS[1], Ebru Oral, PhD[1,2], Orhun K. Muratoglu, PhD[1,2]

[1]Harris Orthopaedic Laboratory, Massachusetts General Hospital, Boston, MA, [2]Department of Orthopaedic Surgery, Harvard Medical School, Boston, MA

Introduction: Periprosthetic joint infection (PJI) is a serious complication of total joint arthroplasty and a leading cause of revision surgery. For chronic PJI of the knee and hip, two-stage revision arthroplasty is the standard of care, with the first stage involving prosthesis removal, thorough debridement, and implantation of a temporary antibiotic-loaded polymethyl methacrylate (PMMA) spacer to preserve joint function and deliver local antimicrobial therapy [1]. However, PMMA spacers provide limited antibiotic release and are prone to wear, debris generation, and mechanical failure during prolonged weight-bearing use [2]. Gentamicin sulfate-loaded ultra-high molecular weight polyethylene (GSPE) was developed to overcome these limitations by combining sustained antibiotic elution with the superior toughness and wear resistance of UHMWPE, warranting comprehensive preclinical evaluation for temporary implantation.

Methods: GSPE underwent extensive biocompatibility testing under the ISO 10993 framework, including in vitro cytotoxicity, intracutaneous irritation, sensitization, acute systemic toxicity, and 4- and 13-week intramuscular implantation studies with comparison to HDPE controls. Chemical characterization was performed using exhaustive extractions and a multimodal analytical platform encompassing mass spectrometry, chromatography, metals analysis, and spectroscopy, followed by toxicological risk assessment in accordance with ISO 10993-17. Mechanical performance was evaluated through compression, impact, shear, tensile, and fatigue crack-propagation testing, both before and after accelerated oxidative aging. Antibacterial efficacy against *Staphylococcus aureus*, *Staphylococcus epidermidis*, and *Escherichia coli* was assessed under planktonic and biofilm conditions, with comparisons to polyethylene and gentamicin-loaded PMMA cement. Gentamicin elution from full-scale tibial and femoral GSPE components was quantified over 180 days. In addition, wear performance was assessed using a force-controlled ISO 14243 knee wear simulation over one million cycles, with gravimetric wear measurements and visual inspection for structural damage.

Results: GSPE demonstrated excellent biological safety across all evaluated endpoints, including cytotoxicity, irritation, sensitization, and systemic toxicity effects. Similarly, no adverse local tissue responses were observed through 13 weeks of implantation. Chemical characterization identified only low-level extractables, all of which exhibited acceptable margins of safety under conservative exposure assumptions. Mechanical testing showed that GSPE maintained robust performance both before and after aging, including compressive strength, impact toughness, tensile properties, shear resistance, and stable fatigue crack-propagation thresholds, which are comparable to those of conventional UHMWPE. Antibacterial testing demonstrated significant reductions in planktonic growth and surface-associated biofilm formation for all tested organisms, with efficacy comparable to gentamicin-loaded PMMA cement, confirming preserved antibiotic activity. Gentamicin elution exhibited an initial burst followed by sustained release through 180 days, with daily elution remaining well below established systemic toxicity thresholds while maintaining therapeutically relevant local concentrations. Knee wear simulation demonstrated linear, load-dependent wear without evidence of cracking, delamination, or fracture. Although femoral components exhibited higher wear rates than tibial components, all values were consistent with expectations for temporary spacers.

Discussion: This comprehensive preclinical evaluation demonstrates that GSPE is a biologically safe and mechanically durable material capable of sustained antimicrobial delivery during prolonged temporary implantation. GSPE addresses key limitations associated with PMMA spacers by combining extended antibiotic elution with superior toughness and wear resistance. Collectively, these findings support GSPE as a promising alternative material for long-term temporary spacers in two-stage revision arthroplasty.

Acknowledgment: This work was supported by the Muratoglu-Harris Endowment.

References: [1] Asik, Mehmet D., et al. "Enhanced antibiotic release and mechanical strength in UHMWPE antibiotic blends: the role of submicron gentamicin sulfate particles." *JBJS* 107.6 (2025): 586-593.
[2] Yang, Fu-Shine, et al. "Mechanical failure of articulating polymethylmethacrylate (PMMA) spacers in two-stage revision hip arthroplasty: the risk factors and the impact on interim function." *BMC musculoskeletal disorders* 20.1 (2019): 372.

Novel Spectroscopic Approaches for Oxidation Index Assessment in UHMWPE Implants

Azita HassanMazandarani[1], Ananya Mathews[1], Petra Baylin[1], William Querido[1], Timothy Wright[2], Nancy Pleshko[1], Aarti Shenoy[2]
[1]Temple University, Philadelphia PA, [2]Hospital for Special Surgery, New York NY
Email of Presenting Author: tul04593@temple.edu

Introduction: Ultra-high molecular weight polyethylene (UHMWPE) wear is influenced by oxidation, which has been a concern for the arthroplasty field. Long-term implant survival remains limited by polyethylene wear, which leads to debris formation, and osteolysis requiring revision surgery.[1] Fourier-transform infrared (FTIR) spectroscopy is the standard technique used to measure polyethylene oxidation based on the carbonyl absorbances centered near 1720 - 1740 cm^{-1} ratio to the 1370 cm^{-1} polyethylene methyl absorbance as demonstrated in previous studies.[2,3] The maximum FTIR spatial resolution is wavelength dependent and on the order of ~ 6 μm. Further, sample preparation requires microtoming thin sections. Optical photothermal infrared (O-PTIR) spectroscopy is a novel method that provides a higher spatial resolution of 500 nm and with non-contact reflection-based detection mode can accommodate thicker samples for assessment. As PE oxidation varies temporally and in response to localized stress, sub-micron oxidation assessment could uncover patterns that would yield insight into oxidation mechanisms. Similarly, spatial distribution of oxidation index (OI) through the samples using FTIR hyperspectral imaging allows clear visualization of oxidation changes within the sample. **This study evaluates OI using O-PTIR as an alternative to FTIR, alongside FTIR hyperspectral imaging.**

Methods and Materials: To investigate OI measurement via O-PTIR as an alternative approach to FTIR, a retrieved patellar component (PC) (revised for right knee osteolysis) was analyzed. Two types of samples were prepared: a 5 mm thick section made using a razor blade, and a 200 μm microtomed section (thin section) from the region adjacent to the thick section. Care was taken to select a component and a region on the component that
did not exhibit delamination resulted from oxidative embrittlement.[4] To illustrate the distribution of OI across the sample using FTIR hyperspectral imaging, a posterior-stabilized knee insert (PS sample) revised for aseptic loosening and tibial post fracture was used. The sample was microtomed to obtain 150 μm slices. Both samples used for this study are compression-molded UHMWPE and part of our IRBapproved institutional retrieved implants collection. The samples were stored in a -4° freezer within 6 months of retrieval. Both samples were boiled in n-heptane to dissolve any penetrating lipids, as is standard for these analyses.[4] FTIR spectral data were collected in transmittance mode as line scans ~ 6.5 – 7 mm in length from the PC thin section starting near the articular surface through to the backside at 6.25 micron pixel resolution with a Perkin Elmer Spotlight 400 imaging spectrometer. OPTIR data were collected as line scans on the same thin section from the same regions for comparison to FTIR data and from the thick section in regions that paralleled those collected on the thin section. The O-PTIR data were collected using a mIRage instrument. Due to inherently polarized O-PTIR laser, 500-micron line scans were collected starting at the articular surface in the thin and thick samples in perpendicular orientations (along X and Y stage axes) to assess orientation effects on spectral parameters. Furthermore, OI mapping through the PS sample was conducted using FTIR hyperspectral imaging at 25-micron pixel resolution. Spectral data were processed in Isys spectral imaging software. The line scans (N = 3 per section/technique) and FTIR hyperspectral images were smoothed and OI was calculated as the ratio of integrated areas of the carbonyl (1730 cm^{-1}) and the methyl (1370 cm^{1}). Data were compared based on trends in the OI values in the line scans.

Results: The overall trend in the OI obtained from the thin section is qualitatively similar for the FTIR and O-PTIR data (Figure 1). The higher OI values are in the same location in both data sets, but the magnitude of the values differ. In the FTIR data, the OI values range from ~0.02 and ~0.32, with little scatter in the data. In the O-PTIR data, the OI values range from ~0.2 to over 2.0, with more scatter in the data. Nevertheless, a significant correlation was found for each data set (Figure 1). The O-PTIR data collected in two orientations from the thin and thick sections also demonstrate similar trends, indicating lack of a laser orientation effect (Figure 2). Additionally, OI mapping provides a better view of localized oxidation (Figure 3).

Discussion: These data demonstrate that O-PTIR can be used to assess oxidation information from UHMWPE implants, with values that parallel those using the FTIR approach. The additional scatter in the O-PTIR data compared to the FTIR data arises from the higher submicron resolution, showing a more granular view of the oxidation variation within the implant material, which are smoothed out in the FTIR data due to the larger data collection regions. The O-PTIR OI values are ~ 10-fold higher than the FTIR OI values, a difference which arises largely from a larger oxidation peak absorbance as opposed to smaller methyl absorbance (data not shown). Additionally, we demonstrated that for these samples, a polarized laser source does not impact the OI values. OI mapping was performed as an innovative method to visualize the distribution of oxidation through the sample.

References:

1. Asher DP, Arthroplast Today, 2024;30:101550.
2. Spece H, J Arthroplasty, 2019;34(12):3088-3093.
3. Currier BH, J Arthroplasty, 2007;22(5):721-731.
4. Nickel BT, JBJS. 2025;107(11): e58.

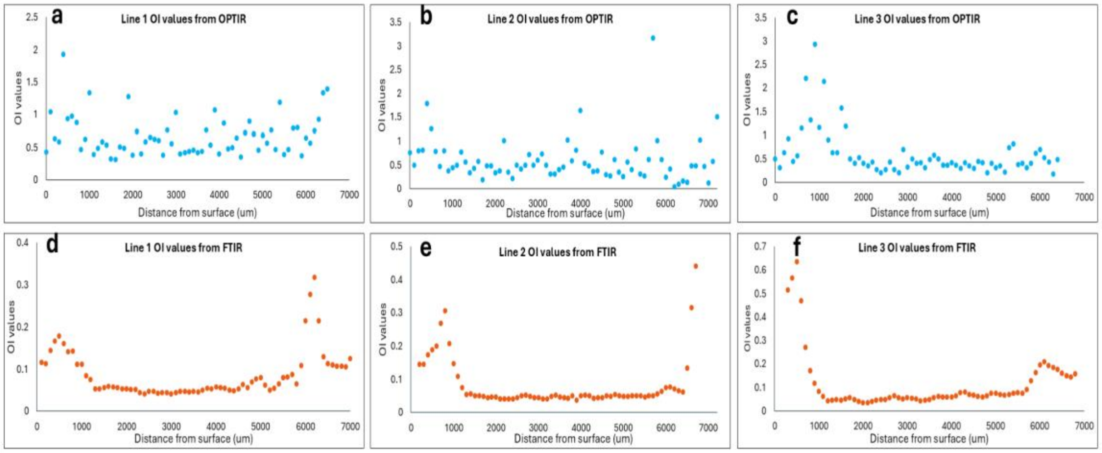

Figure 1: Oxidation index (OI) profiles from three-line scans of a thin section measured by O-PTIR (a-c) and FTIR (d-f), showing spatial variation with distance from the articular surface (0 microns).Some data is cut off in the FTIR scan in panel F as it did not align precisely with the O-PTIR scan of the same line in panel C.

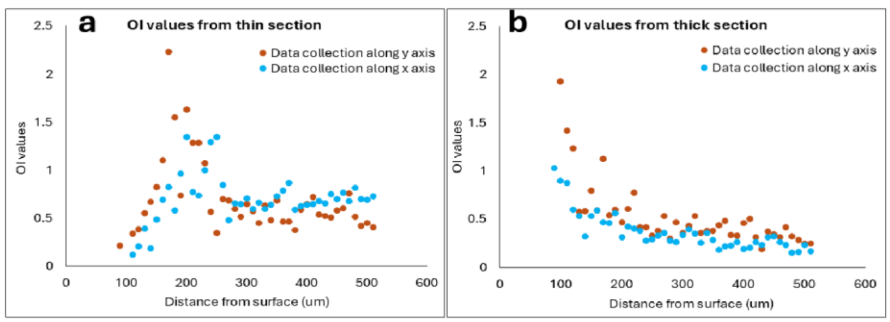

Figure 2: Oxidation index (OI) profiles from the a. thin section and b. thick section collected by O-PTIR, showing polarization effect on OI values variation with distance from the surface. Some data is cut off in the scan from the thick section in panel b as it did not align precisely with the scan of the thin section in panel a.

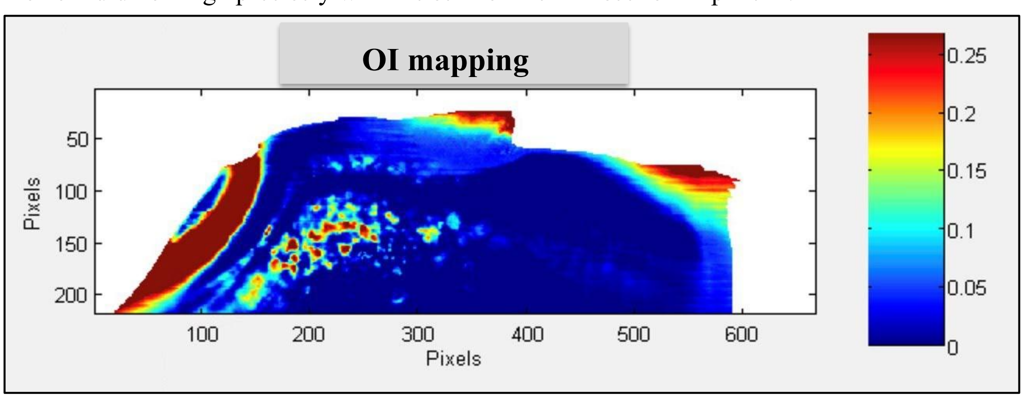

Figure 3: Spatial distribution of oxidation index (OI) at 25 microns pixel resolution across the sample. The maximum OI value is 1.029, with the color scale limited to 0–0.25.

BMSC Extracellular Matrix Formation on PEEK Lattices and a Collagen Membrane Interface

Williams D[1,2]., Gough, J[1,2], Zaribaf, F[3],
[1]Department of Materials, University of Manchester, UK., [2]Henery Royce Institute, University of Manchester UK., [3]Invibio Ltd, Thornton-Cleveleys, UK *Fedra.zaribaf@invibio.com*

Introduction: Focal cartilage and osteochondral lesions of the knee are common and clinically important. Epidemiological summaries report that approximately 5–10% of people over 40 years present with high-grade chondral lesions[1]. Larger and deeper defects are particularly challenging to manage, and current repair strategies may not reliably recreate the cartilage–bone interface, which is critical for long-term durability[2]. Solutions for larger defects should support cartilage regeneration while providing immediate mechanical/structural support to the osteochondral unit. Here, we describe a hybrid concept combining porous polyetheretherketone (PEEK; for biomechanical reinforcement and osseointegration) with a collagen membrane (to support cell attachment and tissue regeneration) in an *in-vitro* defect model intended to restore knee joint function

Methods and Materials: Cylindrical PEEK constructs (diameter (ϕ): 5 mm, thickness: 2 mm) were supplied by Invibio (Thornton Cleveleys, UK) and fabricated with an open lattice structure and pore size approximately 400 µm. A bespoke defect model was designed in Tinkercad (v. 2025) and printed using stereolithography (Formlabs Form 3BL) with BioMed Clear resin. The device comprised a central void (ϕ: 5 mm, depth: 1.5 mm) with channels underneath and tangential (ϕ: 1–3 mm) to facilitate media exchange. Additional L-channels were placed on the top surface (ϕ: 1 mm) for attaching the collagen membrane. Primary human bone marrow-derived mesenchymal stem cells (BMSCs, **PromoCell GmbH**, Germany) were cultured in low-serum MSC media and passaged 1:3 at 80% confluency for a maximum of five passages. At 90% confluency, cells were pelleted, counted with Trypan Blue, and resuspended in fresh media to the required concentration. PEEK constructs were sterilised in 70% ethanol for 2 h, washed in sterile phosphate-buffered saline (PBS), and transferred to a 96-well plate. Collagen membranes (Chondrogide, Geistlich, Switzerland) were marked with a 10 mm cork borer, cut into individual circular pieces, and placed in a 24-well plate. All specimens (PEEK and collagen membrane) were seeded with 1×10^5 BMSCs per specimen and incubated for 24 h. For matrix production characterisation, PEEK samples were incubated for 14 and 21 days. For the in-vitro defect model, PEEK constructs were transferred to a 24-well plate and all specimens cultured for a further 48 h in 1.5 mL media. PEEK constructs were placed into the defect model and a collagen membrane secured cell-side-down on top using suture fixation. Constructs were cultured for 21 days. Samples were fixed in 10% formalin for 20 min and washed in PBS. Assembled PEEK constructs underwent three treatments in fresh sodium borohydride to reduce autofluorescence. Samples were permeabilised, blocked with 2.5% goat serum for 1 h, and treated with goat anti-collagen I (COL I) primary antibody (1:200) for 2 h at room temperature. A donkey anti-goat 488 fluorescent secondary antibody (1:250) with TRITC-conjugated phalloidin (1:500) was applied for 1 h in darkness, and samples were counterstained with DAPI (1:500) for 15 min. Whole-construct imaging was conducted with a CQ1 confocal cell imaging microscope (Yokogawa). Images were recorded as tile stacks with a 9 µm z-height and reconstructed in ImageJ. Constructs for histology were fixed and sent to the University of Liverpool for resin embedding. Samples were infiltrated at 4 °C under vacuum with media for 5 days, embedded in Teflon blocks and left for 3 days to polymerise. Blocks were attached to Perspex for hardening over 2 days, sectioned at 5 µm, and stained with haematoxylin & eosin.

.**Results:** Phalloidin staining revealed that BMSCs adopted an elongated and well-spread morphology, forming a confluent layer on the PEEK constructs which infiltrated the porous lattice. BMSCs on PEEK expressed collagen I COL I at 14 and 21 days. For the defect model at day 21, increased adhesion was evident at the PEEK–collagen interface, indicated by resistance to peeling of the membrane from the construct . Histology demonstrated evidence of union between BMSC populations on PEEK and the collagen membrane with H&E staining revealing the extension of cell bodies between the voids of the PEEK construct and membrane surface .

Discussion: PEEK constructs supported BMSC attachment and spreading and promoted COL I deposition, which may provide a matrix foundation favourable for subsequent osteogenic differentiation and subchondral bone repair[3] . The bridging of BMSC populations between collagen membrane and PEEK indicates a developing physical union between two materials *in-vitro*. Extending the culture duration and implementing quantitative assays will be important to determine the extent of integration and how this influences extracellular matrix deposition over time.

The authors wish to acknowledge the support provided by Geistlich for this project.

1.Orthobullets (2025) *Articular cartilage defects of the knee*. Available at: https://www.orthobullets.com/knee-andsports/3133/articular-cartilage-defects-of-knee (Accessed: 19 February 2026). [orthobullets.com]2. Leal, D.P., Mores, V., Varone, B.B., Gobbi, R.G. and Tirico, L.E.P. (2025) 'Treatment of multiple chondral and osteochondral lesions in the knee: current challenges and treatment gaps for larger and deeper lesions', *Journal of ISAKOS*, Article PIIS2059-7754(25)00545-0.3.Leyh, M., Seitz, A., Dürselen, L., Schaumburger, J., Ignatius, A., Grifka, J. and Grässel, S. (2014) *Subchondral bone influences chondrogenic differentiation and collagen production of human bone marrowderived mesenchymal stem cells and articular chondrocytes*https://doi.org/10.1186/s13075-014-0453-9 . **Arthritis Research & Therapy**, 16(5), p.453.

Commercial Approval of a Fully Polymeric Surgical Mitral Valve

Stanfield, JR[1,2], Grainger, DW[1], Gharib M[3]
[1]University of Utah, Salt Lake City, USA, [2]Foldax, Inc., Salt Lake City, USA, [3]California Institute of Technology, Pasadena, USA
Ryan.Stanfield@Utah.edu

Introduction:
Polymeric materials are redefining surgical heart valve design by offering enhanced durability, biostability, and manufacturing precision. A surgical mitral valve featuring a novel siloxane-polyurethane urea (SiPUU) leaflet material recently achieved commercial approval outside the United States (OUS), marking a significant milestone for polymer-based cardiovascular implants. This device integrates SiPUU leaflets with a polyetheretherketone (PEEK) frame doped with barium sulfate for radiopacity and ultra-high-molecular-weight polyethylene (UHMWPE) sutures for fixation of a polytetrafluoroethylene (PTFE) sewing ring, creating a fully polymeric construct optimized for long-term performance.

Methods and Materials:
SiPUU leaflets were dip-cast as a single, seamless piece directly onto the PEEK frame using robotic automation, eliminating secondary fixation steps. The PEEK frame was compounded with barium sulfate to ensure radiopacity for postoperative imaging. UHMWPE sutures are employed to secure the sewing ring to the frame, leveraging their high tensile strength and abrasion resistance. Accelerated wear testing (AWT) was performed per ISO 5840 standards, and material characterization included biostability and calcification resistance. Clinical evaluation of the polymer surgical mitral valve (SMVR) was conducted through a human trial in India, enrolling 67 patients with one-year follow-up to support regulatory approval.

Results:
SiPUU leaflets demonstrated exceptional durability, completing 600 million cycles without structural failure, surpassing ISO 5840 requirements for surgical valves. Biocompatibility analysis per ISO 10993 confirmed biostability and negligible calcification. The PEEK frame maintained dimensional stability under physiological loading, and UHMWPE sutures exhibited no fraying or creep during fatigue testing. Clinical outcomes from the SMVR trial showed favorable hemodynamics and no valve-related events at one year, supporting successful OUS commercial clearance.

Discussion:
The integration of SiPUU, PEEK, PTFE, and UHMWPE within a single device represents a paradigm shift toward fully polymeric surgical valves. Robotic dip-casting of SiPUU enables precise leaflet geometry and eliminates manual assembly variability, while PEEK's radiopaque modification enhances imaging compatibility. UHMWPE sutures provide robust fixation without compromising durability. Collectively, these innovations deliver a design

Is Point of Care 3D Printing of PEEK Triflange Cups Feasible for Revision THA?

Steven M. Kurtz, Emily Hess, Sarmad Khan, Kelcy Putlock, Johan Vasquez, Dr. James A. Smith, Dr. Maxwell Courtney
[1]Drexel University, Philadelphia, PA

Introduction
Titanium 3D printed triflange cups are an established treatment option for severe pelvic discontinuity, but are costly and, when produced by offsite, involve weeks of surgical delay. 3D printing PEEK at the point of care (POC) has recently been 510k cleared by FDA for cranioplasty to reduce implant cost and time to treatment. We asked in this pilot study whether 3D printed triflange cups from high strength polyaryletherketone (PAEK) polymers like PEEK could be produced with sufficient strength for revision THA and whether annealing could improve cup strength?

Methods
For proof-of-concept, two representative triflange cups designs were developed based on a set of 49 full body CT scans from the public NMDID repository. Triflange cups (n=3 per design) were additively manufactured using an industrial 3D printer (F421) and AM 200 PAEK filament. A second set of cups (n=3 per design) were annealed in an effort to improve strength. A customizable fixture was developed for mechanical testing of the personalized cups, which were loaded to failure in an MTS load frame.

Results
As-printed (non-annealed) polymer cups failed due to deformation followed by layer separation whereas the annealed cups fractured. The ultimate load (mean ± SD) for the two non-annealed triflange cup designs was 10.2 ± 0.02 kN and 11.0 ± 1.9 kN, respectively. After annealing, the strength of the two designs was 2.60 ± 0.44 kN and 10.5 ± 2.7 kN.

Conclusion
The unannealed PAEK cups exceeded the strength published for a titanium 3D printed design (5.4kN, Kang et al, 2024). The promising results of this pilot study demonstrate proof-of-concept and suggest that polyaryletherketone (PAEK) like polymers PEEK may be suitable biomaterials for future triflange cup applications. Additional research is needed to incorporate porosity into the printed designs and further refine the mechanical test model.

CFR-PEEK in Orthopaedic Implants: What the clinical evidence supports, what it still can't answer, and how evidence is translated into use

Spitler CA[1], Beason DP[2], Slowik JS[2], Reed LA[1], Gambill SL[3], Fleisig GS[1]
[1]Department of Orthopedic Surgery, University of Alabama at Birmingham, Birmingham, AL
[2]The American Sports Medicine Institute, Birmingham, AL
[3]Invibio Inc, West Conshohocken PA
Sherri.Gambill@invibio.com

Introduction: High Tibial Ostoetomy (HTO) is a commonly performed procedure shifting the mechanical axis of weightbearing in order to delay unicompartmental gonarthrosis and the need for a total knee arthroplasty.[1] One of the most commonly performed techniques of HTO is the medial open-wedge approach. Medial open wedge osteotomy sites heal by a process known as endochondral ossification, which requires an optimal range of micromotion at the fracture/osteotomy site. It is believed that when attempting to induce secondary bone healing of a fracture or osteotomy, flexible fixation is important, and an implant that closely matches the modulus of elasticity of the bone might improve union rates. Along with material composition, the structural design and geometry of each implant also play important roles in the biomechanical performance. Diffo Kaze et al studied the biomechanical properties of commonly used HTO plates based on their structural design and found that a plate with a wider T-shaped proximal end showed a higher lifespan prior to failure as compared to other plates having narrow T-shaped proximal ends.[2] Given these findings, along with the studies on material composition, it stands to reason that many factors contribute to the biomechanical properties seen with different implant designs. Although the implant material is only one aspect of the design, it represents one of the most important components. Carbon fiber reinforced PEEK plating has several potential benefits when compared to stainless steel and titanium plating. Carbon fiber PEEK plates have decreased stiffness compared to other metals and the modulus of elasticity is much closer to that of bone, thus avoiding stress-shielding and risk of bone resorption.[3] These properties of carbon fiber reinforced PEEK implants make them a valuable biomaterial for orthopaedic use. The purpose of this study was to compare the quasistatic and fatigue properties of titanium and HTO fixation plate design to a similarly shaped carbon fiber design.

Methods and Materials: Twenty 4th generation large left tibiae composite bones underwent a medial open-wedge HTO fixed with titanium plates (n=10) and CFR-PEEK plates (n=10) using titanium screws for both groups. For the quasistatic testing (n=5 per material group), a constant compressive load to failure was applied. Failure was defined as the first notable decrease in the load-deflection curve that also corresponded to video evidence of failure. For the fatigue testing (n=5 per group), an increasing step load was applied at every 20,000 cycles until failure. Differences between Titanium and CFR-PEEK groups were analyzed via two-tailed t-tests, with significance set at $p \leq 0.05$.

Results: Results from quasistatic testing showed higher mean ultimate failure loads in the Titanium group compared to the CFR-PEEK group; however, this difference was not statistically significant ($p=0.16$). Data from the motion analysis revealed a significantly higher ($p=0.039$) lateral stiffness at failure in the Titanium group. The mode of failure for the Titanium group was consistently a defect in lateral-side cortex of the tibia specimen. The mode of failure in the CFR-PEEK group was a defect in the plate itself.

For the fatigue testing, the maximum number of cycles experienced at failure by any specimen was 460200. The Titanium group resulted in a higher mean failure load, but this difference was not statistically significant. Analysis of the motion sensor data showed higher, but again not significantly higher, vertical and lateral stiffness in the Titanium group.

Discussion: The comparative assessment of two similarly-shaped carbon fiber and titanium HTO plates demonstrated minimal differences in stiffness or cycles to failure. Overall, CFR-PEEK plates were noninferior to titanium plates for use in medial opening wedge HTO. The only statistically significant finding was higher quasistatic lateral stiffness in the titanium group. As the use of carbon fiber plating continues to develop, the potential for improved radiographic assessment of bone healing and the ability to match the modulus of elasticity of bone creates intriguing possibilities for improvements in clinical outcomes.

References:

1. Sabzevari S. et al. High Tibial Osteotomy: A Systematic Review and Current Concept. Arch. Bone Jt. Surg. 2016 Jun;4(3):204-212.
2. Diffo Kaze A et al. Biomechanical properties of five currently used implants for open-wedge high tibial osteotomy. J Exp Orthop. 2015 Dec;2(1):14.
3. Hak DJ et al. Use of carbon-fiber-reinforced composite implants in orthopedic surgery. Orthopedics. 2014 Dec;37(12):825-30.

The Road Towards Establishing Clinical Services to Develop and Produce Patient-Specific PAEK Implans in and by the Healthcare Facility at Point-of-Care: the Singapore General Hospital Experience

Tan BWM[1,2], Ramakrishnan SA[1], Tan SY[1], Ee AY[1], Ahamed NMN[1]

[1]3D Printing Centre, Singapore General Hospital, Republic of Singapore

[2]Department of Neuroradiology, Singapore General Hospital, Republic of Singapore *mark.tan.b.w@singhealth.com.sg*

Introduction: The aim of this project was to establish in the Singapore General Hospital (SGH) the first national platform in Singapore to design, develop and produce at point-of-care within and by the healthcare facility patient-specific PAEK (Polyaryletherketone) implants. The project intent was to enable better implant fit and shorter implant deployment times via in-house processes, improve the resiliency of important medical devices from supply disruption, as well as enable R&D translation. The platform would first develop cranial implants using additive manufacturing methods and techniques, and then progress to develop other implants for craniomaxillofacial and orthopedic applications.

Methods and Materials: The SGH 3D Printing Centre (3DPC) was tasked as the entity within the hospital responsible for the project. The SGH 3DPC develops and produces at point-of-care within the healthcare facility patient-specific surgical rehearsal and implant sizing models, sterilisable surgical localisation and reconstruction guides, as well as medical appliances for clinical care using virtual surgical planning and clinical additive manufacturing techniques in line with Singapore national guidelines for manufacturing by the healthcare service licensee for its own patients. Regulatory and service approval between the hospital and the relevant and responsible national authorities was obtained. Biomedical engineers, radiologic technicians and radiologists with relevant prior expertise in manufacturing operations and quality management systems, business development, anatomical model, medical device and PEEK implant design development and production, advanced image segmentation and radiological analysis and interpretation were appointed to the project team.

Training in PEEK cranial implant design and production of the project team members involving image segmentation, implant CAD design, implant support generation, print protocolling and post-processing was performed at and by an academic medical centre with expertise in PEEK implant development and production at point-of-care (University Hospital Basel, Switzerland). The principles involved in PEEK cranioplasty development were employed upon related cases which involved similar design principles e.g. Polymethylmethylacrylate (PMMA) cranial mold design and production as staged capability development.

A suitable 3D printer platform with the capability of producing PEEK implants (3D Systems EXT 220 MED) was identified, procured and installed in a dedicated facility within SGH. Operational and performance qualifications which include production process validation, material validation (i.e. mechanical and biocompatibility property validation as per ISO 527 and ISO 10993), as well as end-product design and performance validation were performed. Based on ISO13485 principles an enhanced Quality Management System (QMS) for implant development building upon the existing QMS system within the 3DPC incorporating factors such as an enhanced risk management plan as well as clinical follow-up and surveillance protocols was developed. Reimbursement and billing structures for the service were also derived.

Results: The projected start date for clinical services is in end-2026.

Discussion: The elements of establishing a clinical service to develop and produce at point-of-care within and by the healthcare facility are described. The SGH 3DPC is currently also exploring options for the development at point-of-care of other implants including those made from PAEK for craniomaxillofacial and orthopedic applications, and aims to develop the knowledge base and capabilities for these future processes.

In-house facility for PAEK implant production at the Singapore General Hospital 3D Printing Centre.

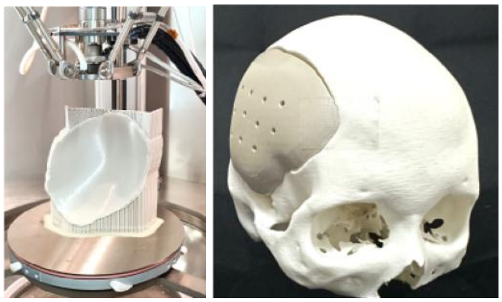

Additive Manufacturing of PEEK Cranial Implants

Evaluating the Static Mechanical Performance of Fused Filament Fabricated Anterior Lumbar Interbody Fusion PEKK and PEEK Devices

Abigail Tetteh
Implant Research Core, Drexel University, Philadelphia PA
aat96@dragons.drexel.edu

Introduction: Implantation of lumbar interbody fusion (LIF) devices or spinal cages is currently the standard of care for alleviating intractable back pain when non-surgical interventions are not successful. To mitigate the risk of spinal fusion failure, biomaterials utilized for spinal cages need to withstand in vivo loading to promote stability and encourage bone ingrowth. Fused filament fabrication (FFF) can be used to process and integrate porosity into high-performance thermoplastics like polyether-ether-ketone (PEEK) and polyether-ketone-ketone (PEKK) to increase the chances of biological fixation. Since PEKK shares many of PEEK's advantageous properties and is less challenging to process using FFF printing, its potential for creating spinal cages was explored.

Methods and Materials: The mechanical performance of FFF-printed anterior LIF PEEK and PEKK idealized cages was evaluated under static axial compression and compression-shear test configurations, following ASTM F2077. The outcomes were compared to the documented mechanical performance of PEEK and metallic LIF devices previously submitted through the FDA 510(k) pathway. Additionally, optical microscopy and micro-computed tomography were used to assess the FFF-printed porous cages' pore size, porosity, and pore space interconnectivity.

Results and Discussion: This study found that both solid and fully porous PEKK and PEEK cages met the 5th percentile benchmarks for axial compression performance (stiffness: 7.7 kN/mm, yield: 10.8 kN, ultimate: 15.3 kN). Additionally, solid cages of both materials met the minimum mechanical requirements for compression-shear (stiffness: 2.2 kN/mm, yield: 4.0 kN, ultimate: 5.0 kN). In contrast, the fully porous counterparts achieved between 65-90% of these benchmarks for PEKK and 72-79% for PEEK. Based on the deformation behavior of the spinal cages, FFF-printed PEKK exhibited greater ductility than PEEK, implying superior interlayer adhesion. All porous cages possessed structural characteristics, such as pore size, porosity, and interconnectivity, that would make them suitable for promoting bone ingrowth.